Delft University of Technology

Wood as a scour protection

MSc Graduation Work

Master Thesis Report

Author:
Laurens Beulink 4076532

Supervisors:
Prof. Dr. Ir. Uijttewaal, W.
Ir. Verhagen, H.J.
Dr. Dionisio Pires, L.M.
Dr. Ir. Bricker, J.D.
Dr. Ir. Sieben, J.

Preface

This thesis is written as part of the master program for Hydraulic Engineering at Delft University of Technology. I would like to thank the Delft University of Technology, as well as Deltares and Rijkswaterstaat for giving me the opportunity to work on a graduation subject that incorporated laboratory model experiments. I would like to thank my graduation committee members on their support and constructive criticism. I would in particular like to thank my daily supervisor Jeremy Bricker, for his guidance throughout the process of graduating. Additionally, special thanks go out to the supportive staff at the Hydraulics Laboratory of the Delft University of Technology, who have assisted me on numerous occasions with their expertise in laboratory measurement techniques and so on. Although the experimentation part is only a relatively small piece of the overall time I have spent at the Delft Hydraulic laboratory, it has still been a great learning experience for future endeavors in hydraulic modeling.

L.M.R. Beulink
Delft, Febuari 2018

Summary

Scour holes are a commonality in rivers and canals, and can under certain conditions form a threat to the stability of nearby hydraulic structures. The practice of repairing and protecting areas under high hydrodynamic loads is a common practice with traditional protection requiring multiple layers of aggregates or large stone structures.

Recently, a new initiative has been brought forward that incorporates scour protection in the form of a layer of logs on top of a traditional filling of sand. This has raised many questions regarding the nature of such a protection. The questions have prompted the creation of multiple research projects, including the study into the response of the bed morphology.

The focus on this study will be the morphology in which experiments will be conducted to form a baseline for additional studies. Experiments conducted for this thesis will focus on the creation of a scenario were clear water scour generates the development of a scour hole. This is done by gradually constricting the flow width in a laboratory flume, causing a higher erosivity in the constricted sections.

These experiments consist of experiments without logs, to form a comparable basis, experiments with a single log and experiments with multiple configurations of protection. Scour development is monitored with laser equipment. Near bed flow conditions are measured with an acoustic Doppler at predetermined locations. Beside these quantative measurements, images and video footage is taken.

It is concluded that the experiments without logs behave like was expected, scour forms in the area that is constricted and scour moves upstream. Theoretical scour depths were not reached, but were approached. Experiments with single logs, showed that depending on the flow conditions, logs have the tendency to cause scour and under certain flow conditions will turn perpendicular to the governing flow direction. The experiments incorporating a layer of logs placed on the bed in the constricted area showed varied activation mechanisms and results. In general the logs have had the tendency to reduce scour rates by 40-50 %.

A log layer in which the logs are placed parallel to the governing flow direction offer the most resistance to being displaced, but cause scour to form underneath the upstream located faces. This scour hole is able to penetrate very deep and very fast into the surface, attaining scour depths reached in the basic experiments within 24 [h] that took experiments without logs 96 [h]. A log layer in which the logs are placed perpendicular to the governing flow direction have less resistance to moving, given the bed is flat. Scour develops as a uniform trench underneath the most upstream located log, but because of the perpendicular placing of the logs, logs can easily roll into the formed scour hole and obstruct the continued scour underneath the logs.

Comparing all experiments, one can conclude that the logs placed perpendicular to the governing flow direction show impressive results, reducing scour rates by 50% and lowering the maximum scour depths by 10%. Additional scour mechanisms do arise, but these are seen as negligible as the proposed application program for logs avoid the cause for generation of these scour holes. Additionally to this specific set of experiments, a layer of logs placed perpendicular to flow can protect areas under tidal regimes due to the specific mechanism that occurs with flow perpendicular placed logs.

Contents

I Introduction

I.1 Background

Both naturally occurring and also human induced scour and erosion are a threat to many of the hydraulic works that are often present in the direct vicinity of rivers, canals and other bodies of water. Examples of these scouring holes can be seen in Figure 1. As the ongoing mission of the Dutch organization Rijkswaterstaat is to protect the inhabitants of the Netherlands against floods and keep the waterways accessible for shipping and other vital functions, maintenance of the waterways is a necessary evil.

Until now maintenance was conducted in more traditional fashion, by either traditional bottom protection or dredging works, but new legislature from the Dutch government focusing on improving the biodiversity, called: the water framework directive (Kader Richtlijn Water in Dutch), has presented an opportunity to approach multiple issues at once.

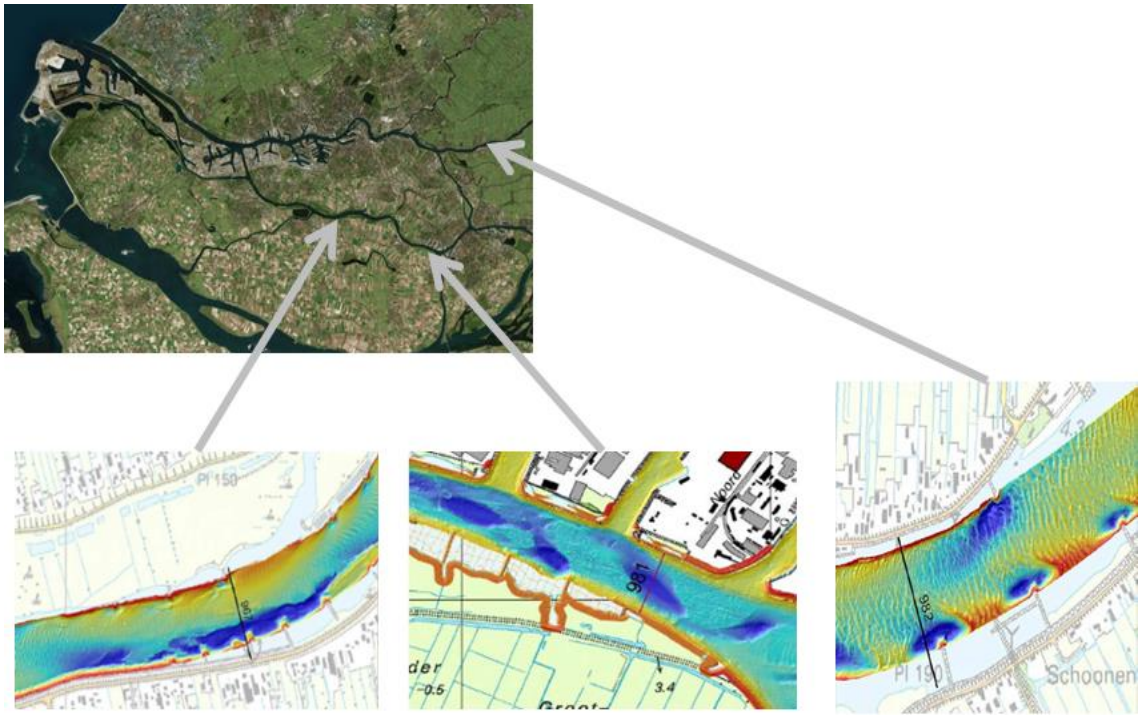

Figure 1; Examples of possible locations

As a matter of flood protection, trees and other obstacles are generally removed from floodplains, in order to improve peak discharge. Until now these trees have had no other use. As a measure to improve bio diversity, placement of these cut trees in sheltered areas of rivers and other bodies of water seem to be a prudent way to provide underwater flora and fauna more space to reside. The logs will saturate over the course of several months/years and eventually sink to the bottom. The cycle can then be repeated with new wood while the old logs can and must be removed.

After this point the logs would then be reapplied as a biological bottom protection for the before mentioned scouring holes. This means the logs can generally be reused at locations close to the site of the improved flora and fauna, which saves transport and provides a use case for these left over logs.

The concept of the scour protection would incorporate filling pre-existing scour holes with filler (sand & aggregates), and covering this scour hole with a layer of reused logs. A visualization of this application can be observed in Figure 2. At this point Rijkswaterstaat is primarily looking for test locations for application in the “Oude Maas” (Figure 1), but when proven successful other locations might also come under consideration.

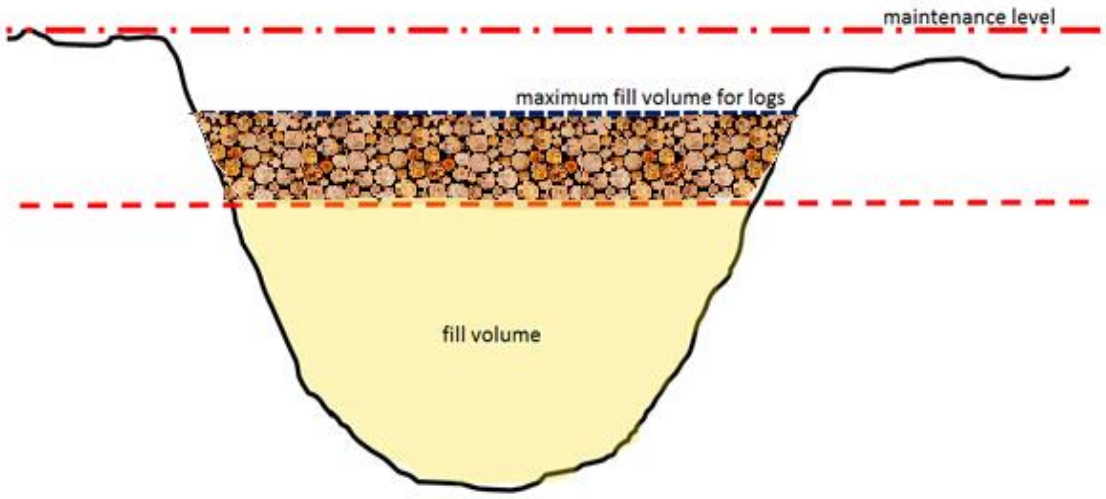

Figure 2; Functional wood (Rijkswaterstaat 2016)

I.2 Problem description

The application of logs in this fashion is relatively undiscovered territory, and questions have arisen regarding the behavior of a protection of logs. Research regarding the topic has been split into three separate sections. Firstly the behavior as a habitat in the sheltered areas of a river is investigated by Deltares.

Secondly research regarding the stability of logs in varying flow conditions has been investigated by bachelor students at the Delft University of Technology (Haage and Çete 2016) & (van Olst, van Leeuwen and van der Scheer 2016). With these studies an outline of suitable flow conditions were determined.

The Third stage regards the morphological response of the river bed to placement of logs, this research study will form the foundation of the third stage, with additional research being conducted by other Master students in the near future.

I.3 Research Objective & Questions

The primary goal of this master thesis is to obtain a better understanding concerning the effect of the placement of logs in scouring holes. This research study will build upon previous studies conducted by (Haage and Çete 2016) & (van Olst, van Leeuwen and van der Scheer 2016) and the recommendations that where specified in the given sources. The primary research question holds:

"What is the effect of the placement of logs as bottom protection, on the in time development of scouring holes?"

In the light of this question it was decided that laboratory experiments should form the foundation of this research study, this is later more thoroughly discussed in section I.4 Methodology. Thus secondary questions that will be important to the stated primary research question are:

How do scour quantities develop in a chosen laboratory model without the application of logs, and does this concur with the expectations from the hydraulic sciences?

What is the behavior of a single log on itself and the bed in varying flow conditions?

What matter of log protection application is most appropriate in this model, and how does certain application affect the development of the scour quantities.

Does the scouring process change in such a way that new scouring mechanisms arise and/or start to dominate the scouring process?

I.4 Methodology

There are essentially two ways of obtaining insight into real world processes excluding field measurements and investigation. These are respectively physical modeling and numerical modeling. The applicability of numerical modeling is highly dependent on the existing knowledge and insight into hydraulic processes. There is a large amount of pre-existing knowledge available concerning scouring around objects, but this usually describes pier like objects, that extend throughout the entire water column. Alternatively, there is knowledge into scour around pipelines, but this primarily describes scour due to flow perpendicular to the direction of the pipelines. The issue at hand combines parts of both scouring mechanisms, and thus it is decided that the construction of a physical model is an important first step in obtaining insight in this combined effect.

II Background and Theory

II.1 Characterization of flow

From the hydraulic sciences two dimensionless numbers are known and used in order to describe the state of flow of a body of water. These numbers are called the Froude number and the Reynolds number.

II.1.1 Froude number

The Froude number is a description of the state of flow and represents the ratio between inertia and gravitational forces. Under this description flow can be distinguished into three separate states namely:

$Fr < 1$	$Fr = 1$	$Fr > 1$
Sub-critical flow	critical flow	super critical flow

While sub critical and super critical states offer an array of possibilities, critical flow has only a single possible flow velocity (u) for a specific depth (or vice versa). Generally speaking, the Froude number tells us whether or not information, in the form of waves, can propagate upstream. The Froude number is written as follows:

Equation 1; Froude Number

$$Fr = \frac{u}{\sqrt{gL}}$$

$\boldsymbol{u}$ = $\boldsymbol{flow\ velocity}$ $[\boldsymbol{m/s}]$
g = $gravitational\ acceleration$ $[m/s^2]$
L = $length\ scale$ $[m]$

II.1.2 Reynolds number

The Reynolds number is also a very common ratio applied in scaled experiments. It describes the ratio between inertial forces and viscous forces. Under this description flow can be distinguished into roughly states namely:

$Re < 2000$	$2000 < Re < 4000$	$Re > 4000$
Laminar flow	Transitional flow	Turbulent flow

Generally speaking, the Reynolds number describes the significance of the viscous forces of the water and whether or not turbulence is a phenomenon that will or will not occur. The Reynolds number is written as follows:

Equation 2; Reynolds Number

$$Re = \frac{uL}{v}$$

$\boldsymbol{v}$ = $\boldsymbol{kinematic\ viscosity}$ $[\boldsymbol{m^2/s}]$

II.2 Flow - Stability

The focus of this section will be to present the reader with a background into the stability of loose and non-cohesive grains in uniform flow conditions. Although sediment transport and scour are very broad subjects and have a wide variety of factors that contribute to the movement of particles, the basis for scour is presented in this section.

II.2.1 Shields

From the hydraulic sciences understanding the forces acting on a bed and even individual grain has been given a significant amount of attention in the past. Basically two ways to approach this problem have been widely accepted. Namely the Shields and the Izbash approach. The Izbash approach considers forces acting on an individual grains and tries to determine the balance of these forces. The shields approach considers the moving water to exert a friction force on a bed. For larger individual boulders and rocks the Izsbash approach has in the past generally proven to be more effective, while for smaller grains the application of the shields approach is seen as more intuitive. The shields criterion is defined as following:

Equation 3; Shields parameter as function of the dimensionless bed shear stress

$$\Psi_c = \frac{\tau_{bc} * d^2}{(\rho_s - \rho_w) * g * d^3} = \frac{u_{*c}^2}{\Delta * g * d}$$

τ_{bc} $= critical\ shear\ stress\ [N/m^2]$
d $= grain\ diameter\ [m]$
ρ_s $= density\ soil\ [kg/m^3]$
ρ_w $= density\ water\ [kg/m^3]$
u_{*c} $= critical\ shear\ velocity\ [m/s]$

The Ψ parameter becomes the mobility parameter when actual velocity and grain parameters are used and can thus be used to describe stages of sediment transport (further addressed in section 2.2.3)

Reynolds Particle number

The Reynolds particle number is an important concept that tells us whether or not a particle protrudes into the turbulent boundary layer or stays within the viscous sub-layer. This value strongly depends on flow velocity and particle diameter. When the value is larger than about 400, particles protrude beyond the viscous sub layer, which tells us that flow around the particles is turbulent. The Reynolds particle number is defined as follows:

Equation 4; Reynolds particle number

$$Re_* = \frac{u_{*c} * d}{v}$$

Transport modes

With the shields parameter defined, 7 stages of particle transport were empirically defined and portrayed as a function of the shields parameter and the Reynolds particle number or the dimensionless grain size. A diagram plotting shields as a function of dimensionless grain size can be seen in Figure 3.

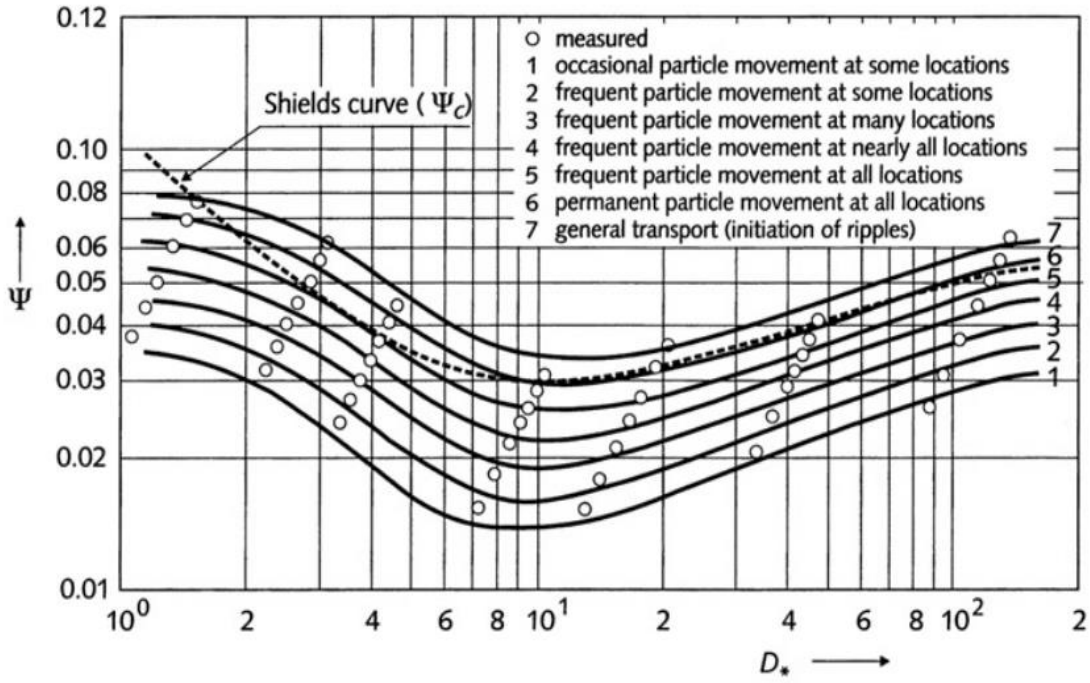

Figure 3; Modified Shields diagram plotting the Shields parameter ψ as a function of dimensionless grain size D* (Hoffmans and Verheij 1997)

The stages of sediment transport are thus defined as follows:

0. No movement at all
1. Occasional moment at some locations
2. Frequent movement at some locations
3. Frequent movement at several locations
4. Frequent movement at many locations
5. Frequent movement at all locations
6. Continuous movement at all locations
7. General transport of the grains

II.2.1 Van Rijn

A method to determine bed load transport rates was proposed by Van Rijn (1984, 1993) This simplified formula for bed-load transport in current only conditions, reads as:

Equation 5; Depth integrated bed load transport

$$q_b = \alpha_b * \rho_s * u * h * (d_{50}/h)^{1,2} * (M_e)^{\eta}$$

q_b $= depth\ integrated\ bed\ load\ transport\ [kg/s/m\ ]$
M_e $= (u - u_c)/(s-1) * g * {d_{50}}^{0,5}$ [-]
ρ_s $= density\ soil\ [m]$
ρ_w $= density\ water\ [m]$
s $= \rho_s/\rho_w\ [-]$
u $= depth\ average\ velocity\ [m/s]$
u_c $= critical\ deptg\ average\ velocity\ [m/s]$
α_b $= emperical\ coefficient\ (0{,}015)[-]$
η $= emperical\ coefficient\ (2{,}4)[-]$

The only unknown in this equation is the u_c, this can be computed with the approach proposed by (Soulsby 1997), from this Equation 6 & Equation 7 follow. These equations will later help to predict scour rates.

Equation 6; Critical velocity

$$\mathrm{u_c} = 5{,}75 * \left[\log\left(12 * \frac{h}{6 * d_{50}}\right)\right] * \left[\theta_{\mathrm{cr,motion}}(s-1) * g * d_{50}\right]^{0,5}$$

Equation 7; Shields parameter for critical motion

$$\theta_{\mathrm{cr,motion}} = 0{,}3/(1 + d_*) + 0{,}055 * (1 - \exp(-0{,}02 * d_*))$$

One critical note to make is that the formula utilizes average velocity as a parameter, which is a simplification of the underlying science that links bed shear stresses to average flow velocity through depth. In the formula the transport parameter M_e can be rewritten to bed shear stresses, which are more applicable in situations where flow is disturbed through the presence of a structure.

Equation 8; Transport parameter rewritten for bed shear stresses

$$M_e = \left(\left(\frac{\tau_b}{\rho g}\right)^{0,5} - \left(\frac{\tau_{b,cr}}{\rho g}\right)^{0,5}\right) C/((s-1) * g * d_{50})^{0,5}\ [-]$$

II.3 Scour

II.2.1 Scour Definition

The process of scour can be described as erosion of the surface due to a lack of sediment transport from upstream of the flow direction. There are basically two modes of scour. Either the flow upstream lacks the capacity to transport sediments (Clear-water scour). Or the area considered has a higher transport capacity than the upstream flow (live-bed scour).

II.2.2 Gradual constriction Scour

Whenever a canal or stretch of river narrows, an increase of sediment transport capacity and thus bed erosion is obtained. The new equilibrium depth of the narrow section is larger and a simple equation for the new equilibrium depth can be found by combining continuity equations as stated in (Schiereck and Verhagen 2012). This equation is stated as following:

Equation 9; Discharge continuity

$$Q = B_1 u_1 h_1 = B_2 u_2 h_2 \rightarrow u_2 = \frac{u_1 (B_1 h_1)}{B_2 h_2}$$

Equation 10; Sediment transport continuity

$$S = B_1 k u_1^m = B_2 k u_2^m$$

Equation 11; Equilibrium Depth

$$\frac{B_1^{m-1}}{B_2^{m-1}} = \frac{h_2^m}{h_1^m} \rightarrow \frac{h_2}{h_1} = \left(\frac{B_1}{B_2}\right)^{\frac{m-1}{m}}$$

m $= emperical\ parameter\ [-]$
h $= water\ depth\ [m]$
B $= water\ width\ [m]$

II.2.3 Pier Scour

Of the detached bodies, a pier like structure is one of the best known structures around which scour tends to develop. Consequently, much is known about this phenomenon. The basic understanding is that down flow occurs in front of the object. This down flow together with turbulences generated to the sides and behind the object generates erosion around the detached body.

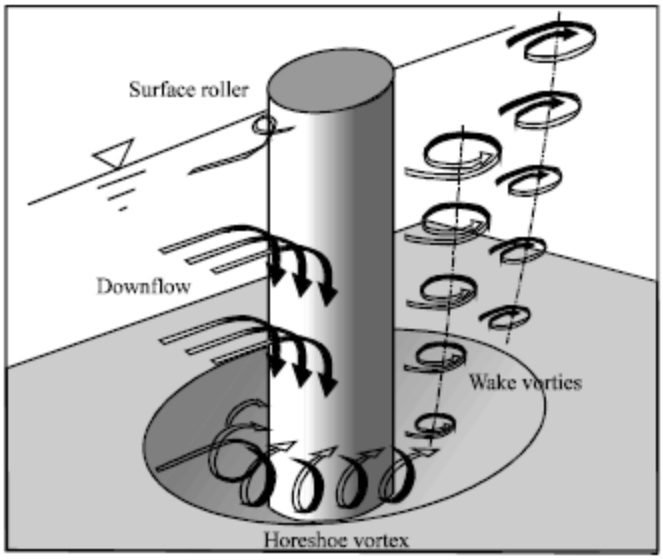

Figure 4; Pier scour figure (Melville and Coleman 2000)

It appears that for slender objects with a water depth/diameter ratio of 2-3, scour depth is mostly proportional to the pier diameter. For wider objects this proportionality does not seem to apply. The maximum scouring depth can be approximated with the following formula:

Equation 12; Pier scour depth general formula

$$\frac{d_s}{D} = 2 * K_S * K_\alpha * K_u * \tanh\left(\frac{h_0}{D}\right)$$

$d_S = scour\ depth$
$K_S = Shape\ factor$
$K_\alpha = Angle\ of\ attack\ factor$
$K_u = Velocity\ factor$

There are however many more pier scouring formulations, that have been developed by researchers from all over the world. A summary of many of the best known formulae can be found in (Sterling Jones n.d.).

II.2.4 Pipeline Scour

Erosion around pipelines is primarily well known for flow perpendicular to the direction of the pipeline itself. Erosion and scour around pipelines can be divided into either scour underneath a pipeline or lee-wake erosion.

Onset of scour

In a steady current the onset of scour below a pipeline is formulated as follows:

Equation 13; Pipeline scour general formula (Mutlu Sumer and Fredsøe 2005)

$$\left\{\frac{\partial p^*}{\partial x^*}\frac{U^2}{g * D * (1-n)(s-1)} + R\right\}_{cr} \geq 1$$

$$p^* = \frac{p}{\rho U^2} \qquad x^* = \frac{x}{D}$$

$s = specific\ gravity\ of\ sand\ [-]$
$n = porosity$ [-]
$x = distance\ along\ perimeter\ [m]$

The R term in this formula is a non-dimensional term, and is included to represent the effects of other mechanisms than the pressure gradient force. Both $p^*, x^*$and R are a function of burial depth to pipe diameter. This means that the more a pipeline is buried, the higher flow velocities are required to initiate scour.

Tunnel erosion

The onset of scour below a pipeline is followed by so called tunnel erosion. When a gap has formed underneath the pipeline, water is diverted through this gap, which significantly increases shear stresses and causes further erosion along the length of the pipeline. As a small increase in bed shear stress causes an even larger factor of sediment transport, once initiation of scour has occurred tunnel erosion occurs rather violently.

Lee-wake erosion

Tunnel erosion is followed by a stage called lee-wake erosion. As tunnel erosion occurs rather fast a dune behind the pipeline is formed. This dune tends to move downstream of the pipeline, but this process takes significantly longer than the initial tunnel erosion. This stage of erosion is governed by vortex shedding behind the pipeline

II.4 Scaling & Scale effects

Scaling Laws

In section II.1 and II.2 the Froude and Reynolds dimensionless numbers were discussed. As stated before the Froude number is a measure of the gravitational forces while the Reynolds number depicts a measure of the viscous forces on flow. When scaling down from a full size prototype or scenario to a model these relationships cannot be valid simultaneously, given the same fluid is used.

Equation 14; Froude Scaling

$$Fr = \frac{u}{\sqrt{gL}} \rightarrow \frac{n_u^2}{n_g n_L} = 1$$

Equation 15; Reynolds Scaling

$$Re = \frac{uh}{v} \rightarrow \frac{n_u n_h}{n_v} = 1$$

As one cannot easily replace the model fluid, one must either choose to adhere to the Froude or Reynolds scale and accept scale errors. In certain scenarios, adhering to the Froude scale will still result in conditions which can be considered turbulent and thus the effect of the scale errors with respect to Reynolds are limited. By keeping the Froude number similar in model as in prototype Froude scaling can for example be used to correctly scale the following hydro dynamical quantities:

- Time scales as $N_t = N_l^{0.5}$
- Current speeds scale as $N_U = N_l^{0.5}$
- Current drag coefficients in rough turbulent flows are identical in model and prototype
- Bed shear stresses in rough turbulent flow scale as $N_\tau = N_U^2 = N_l$

This does however require that the bed material is geometrically scaled to fit the model scale.

Sediment transport

Within the context of this research scaling of the bed material is prone to two considerations, namely sediment transport in general, and scour produced by objects on the bed. The possibility to adjust the scale model bed material opens a degree of freedom which must be dealt. One can obtain similar sediment transport modes by retaining a similitude of shields parameter.

Equation 16; Shields sediment transport scaling

$$\Psi_c = \frac{\tau_c d^2}{(\rho_s - \rho_w) g d^3} = \frac{\tau_c}{(\rho_s - \rho_w) g d} = \frac{\rho u_{*c}^2}{(\rho_s - \rho_w) g d} \quad \rightarrow \quad n_\Psi = \frac{n_i n_h}{n_{\rho s - \rho w} n_d}$$

Equation 17; Reynolds Particle number scaling

$$Re_* = \frac{u_* d}{v} \quad \rightarrow \quad n_{Re*} = n_{u*} n_d = n_\tau^{\frac{1}{2}} n_h^{\frac{1}{2}} n_d$$

It is thus possible to tailor the sediment transport specifically to the size of the model bed material particulates. Alternatively, different materials could be used to replace the model bed material, but this causes extra discrepancies and is thus not further investigated.

Scale effects in pier scour

The lack of agreement between field measurements concerning scour around bridge piles and model experiments is attributed due to a difference in the B/D_{50} ratio in model experiments versus real life conditions (in which B stands for pier width). A smaller ratio of B/D_{50} tends to impede the scour process (Lee and Sturm 2009). Two formulae that have been determined empirically are presented as follows:

Equation 18; Scour depth as a function of pier width to median grain size

$$\frac{d_s}{B} = 5.0 \log\left(\frac{B}{D_{50}}\right) - 4.6 \qquad 6 \leq B/D_{50} \leq 25$$

Equation 19; Scour depth as a function of pier width to median grain size

$$\frac{d_s}{B} = \frac{1.8}{\left(\left(\frac{0.02B}{D_{50}}\right) - 0.2\right)^2 + 1} + 1{,}3 \qquad 25 \leq B/D_{50} \leq 10000$$

$d_s = equilibrium\ depth\ scouring\ hole\ [m]$
$B = width\ bridge\ pier\ [m]$
$D_{50} = median\ sediment\ diameter\ [m]$

These two formulae only hold for situations where the Froude number is below 0.4 and B/D_{50} is not smaller than 20, as this was seen as an uncommon condition for bridge piers to experience. Interestingly enough it appears that when the B/D_{50} reaches about 200 or higher, the ratio of d_s/B no longer changes

III Laboratory set-up & Test Program

In this section, important choices regarding the nature of the laboratory experiments will be discussed. These choices are of importance to develop a working model, and are made to inform the reader of the reasoning behind them.

III.1 Laboratory Model - General

III.1.1 Type of experiment

The first step of the project was to conceptualize an approach to discovering the merits of applying logs as scour protection. The initial concept was to create a clear water scour scenario with the help of a constriction of flow. This creates a situation where an upstream supply of sediment is eliminated as a variable while still experiencing scour at a designated location only.

III.1.2 Scale & Scale relation

Secondly it was decided to design the laboratory set-up to a scale factor of 1:10, and adhere primarily to Froude scaling. This scale was chosen as it is the largest scale the flume could easily accommodate given requirements from Rijkswaterstaat regarding bed material and tree size (Rijkswaterstaat 2016). From existing literature it was found that keeping the scale as large as possible would reduce scaling errors and allow for an experiment with representative results. (Sutherland and Soulsby 2010). The choice of scale relation was made with respect to the processes at hand, as the Froude scale would preserve how forces act on bed materials. Other scale relationships, like the Reynolds relationship, also provided limitations of the flow parameters such that for the designed experiments flow could still be considered turbulent or rough-turbulent and would therefore give representative results to real world processes.

III.1.3 Bed Material

The choice of bed material was driven from considerations with regard to scale errors. The choice of the 1:10 Froude scaling method would require the bed material to be scaled down similarly as the rest of the experiment. This was supported by preceding studies with respect to pier-scour experiments, where a strong relation was underlined regarding the pier width to sediment grain size ratio (Ettema, Melville and Barkdoll, Scale Effect in Pier-Scour Experiments 1998). As it was stated by Rijkswaterstaat that the rivers considered for this project had on average a D_{50} of 300 [µm] (Rijkswaterstaat 2016), a sediment size of 30 [µm] would have been the most appropriate. This sediment size is however so small that electrochemical forces would start to seriously influence and thus disturb the results (Sutherland and Soulsby 2010). It was therefore chosen to work with the smallest acceptable sediment class and accept these scale errors. This sediment class was named AF100 with a D_{50} of 130 [um] (Sibelco 2017).

III.1.4 Model logs

The model logs were fabricated to specifications stated by Rijkswaterstaat (Rijkswaterstaat 2016). With a 1:10 scale, a diameter of roughly 5 [cm] and a length of 50 [cm] were selected. A specimen can be seen in Figure 5.

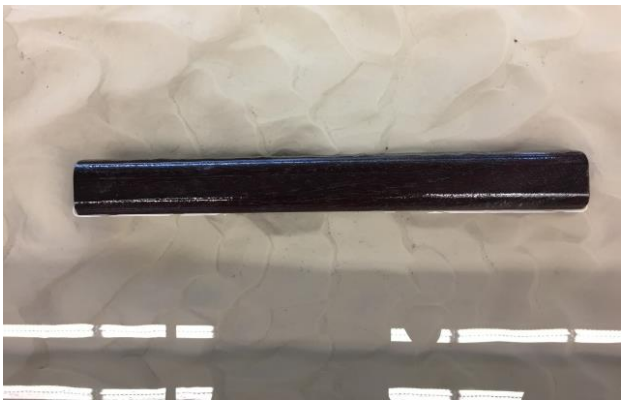

Figure 5; Specimen model tree

According to (Rijkswaterstaat 2016) the specified saturated trees have an estimated density of roughly 1100 [kg/m^3]. The wood used for the fabrication of the trees would therefore have to be at least dense enough to stay submerged. As previous studies conducted by (van Olst, van Leeuwen and van der Scheer 2016), specified azobe to fulfill these requirements, the choice was made to fabricate the model logs from this species of wood.

III.1.5 Laboratory model design

With these basic assumptions in mind it was decided to construct a gradual constriction in the sediment flume of the Hydraulics laboratory at the department of civil engineering and geosciences of the Delft University of Technology. The choice of this type of experiment was made so that a situation could be created in which near zero transport capacity existed outside of the constriction, but at the constriction scour would occur, thus creating a so called clear water scour scenario. Upper and lower limits to the magnitude of constriction were determined. The lower limit originated from obtaining at least a shields type 6 or 7 transport stage at the constriction, but a type 1 or lower transport stage outside of the set-up. Before this could happen, a depth had to be estimated. As the flume was about 80 [cm] deep and early estimation led to believe the thickness of the bed had to be about 20 [cm], it was decided to assume a flow depth of 40 [cm] on top of the artificially created bed so that there was room to tweak either one or both.

After assuming both a flow depth and bed material, it was calculated with the methodology of shields (Schiereck and Verhagen 2012) that 20 [cm/s] was permissible for shields transport not exceeding stage 1 and 30 [cm/s] would amount to approximately stage 6-7. This led to the lower bound requiring the gradual constriction to be about 1.5 times narrower than the full width of the flume. The upper boundary required the logs to be placed perpendicular to the governing flow direction. As the logs were 50 [cm] in length the constriction could not be narrower than that. Both conditions could be fulfilled simultaneously with a constriction of 52

[cm] with respect to the full width of the flume. The resulting design is visible in Figure 6 & Figure 7.Figure 7

To avoid the generation of excessive turbulence at the entrance point of the laboratory set up, the bottom of the flume was elevated over a meter before the entrance point of the laboratory set-up and gradually lifted over another meter in front of that. Locations of interest were appointed so that measurements could be made at these points. To reduce the amount of time required for measuring locations 7-8-9-10-11 were taken so they could be mirrored towards the other side of the laboratory model, thus saving measurement time.

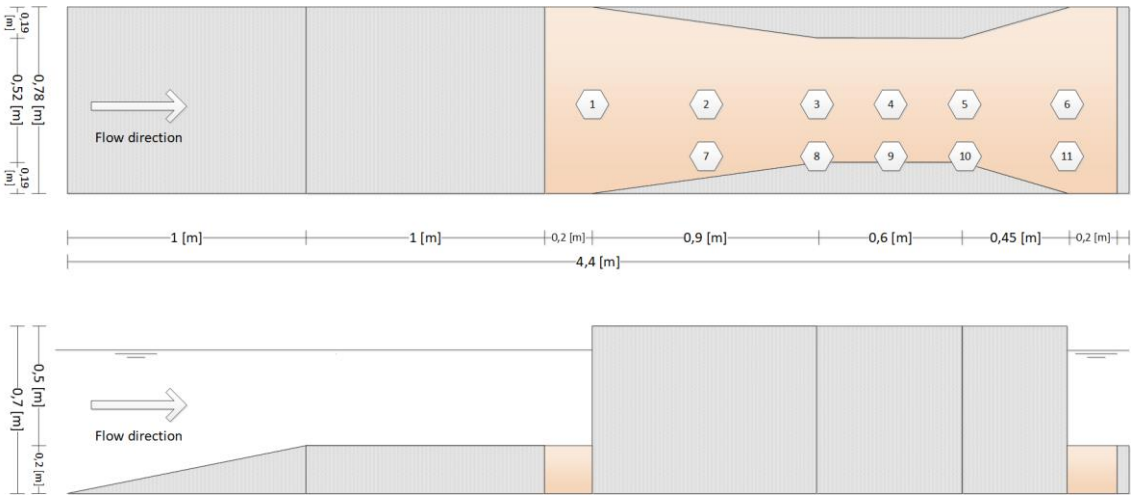

Figure 6; Gradual Constriction Design, woodwork marked grey, sand marked orange

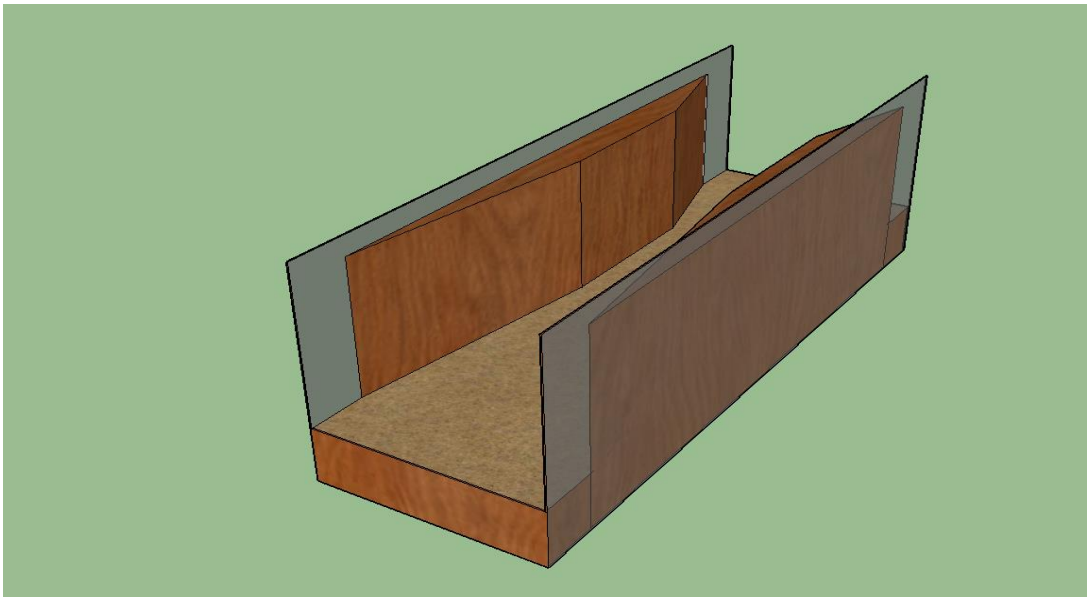

Figure 7; Impression contraction

III.2 Laboratory Model - Equipment

The equipment required for this experiment is driven from by the processes to which insight and deeper understanding is requested. This is further explained in the method section.

III.2.1 Discharge measurements

To measure discharge a Proline Prosonic Flow 91W ultrasonic flow meter (Figure 8) is mounted on the return pipe underneath the flume. With the help of the flow meter average discharge through the pumping system was determined.

III.2.2 Bed & water level surface measurements

Two lasers where used for measurements taken during the experiments. The lasers have separate operating parameters. These operational parameters can be found in Table 1. The short range laser is used for measuring the water level. It thus must be placed within its operating range above the water surface. To provide for a reflective surface, a short piece of white paper is hung just upstream of the laser (Figure 9). The long range laser is mounted within a small boat with a glass bottom Figure 9. Due to its longer range, it is better suited to measure the distance of the bed through the water. The mount of the long range laser is able to move perpendicular to the flow direction, allowing the measurement of longitudinal transects across the entire width of the flume.

Table 1; Operational Parameters Laser equipment (Micro-Epsilon Messtechnik 2018)

Model	Min-range [mm]	Max-range [mm]	Resolution [µm]	Measuring rate [Hz]
Short range (ILD 1302- 200)	60	260	25	750
Long range (ILD 1700- 500)	200	700	30	2500

Figure 8; Proline Prosonic Flow 91W discharge measuring tool (Stenfert 2017)

Figure 9; short range laser in combination with reflective floating paper (Stenfert 2017)

Figure 10; long range laser mounted inside a boat, with a clear glass bottom

III.2.3 Velocity measurements

To measure flow with the possibility of performing complex flow pattern measurements a vectrino profiler produced by Nortek is used. This device applies acoustic Doppler velocimetry to determine the flow velocities in three directions. The vectrino acoustic Doppler can measure up to a sample rate of 100 [Hz]. It has a measuring range of 30[mm] starting 40 [mm] from the transmitter. This range can be in a resolution of cells of 1/2/3 or 4 [mm]. Additionally, the device can measure distance to the bottom which could be helpful during measurements. Requirements for measuring include a signal to noise ratio of 15 or above. As the water used can be made turbid with clay particles this should not be a problem, but will be monitored closely nonetheless. Additionally, measured velocity values should have a sufficient correlation. It is assumed that a correlation of above 90% should meet the requirements with respect to the quality of the measurements. A in transverse direction movable pulley device, mounted on a movable cart, is used to lower and displace the vectrino to desired locations (Figure 11)

Figure 11; Vectrino (black cylinder marked 2), attached to a pulley device, mounted on a movable cart

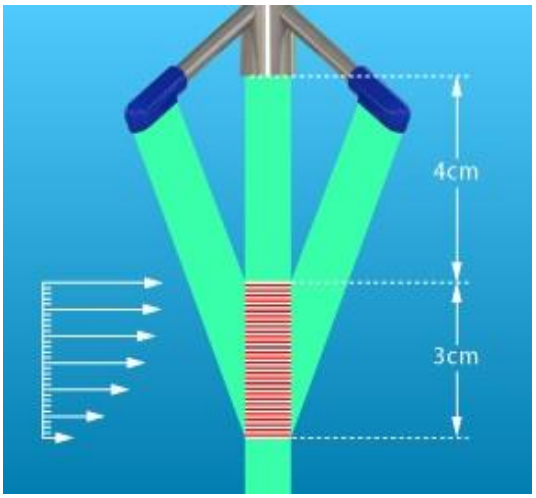

Figure 12; Concept of the Vectrino Profiler (NortekUSA 2018)

III.2.4 Additional Equipment

Three additional pieces of equipment were used during experiments. A so called “pulse-wheel” is used in combination with the long range laser to couple measured input by the laser with a spatial coordinate. This is done with the second piece of equipment, namely a measurement pc equipped with Dasylab & Matlab. The third piece of equipment was a personal video camera to take video imagery of the experiments.

III.3 Test Program

Following the preparation phase, a series of experiments were designed and proposed. Basically the experiments can be subdivided into three categories namely experiments with no logs, with a single log, and with a cover of logs. A summary of all experiments is found in Table 2.

III.3.1 No logs A.K.A Basic Scour

The experiments with no logs, called Basic Scour experiments, focus on generating gradual constriction scour only. The results of these experiments will form a reference point to any follow up experiments with logs and possible follow up research for other students. In total this experiment will be conducted three times. The conditions for flow have been calculated according to the shields theorem. The procedure for the determination of these values is discussed in Appendix III

III.3.2 Single log A.K.A Burial Scour

The experiments with a single log, called Burial Scour experiments, focus on the behavior of the bed and the log in a multitude of flow conditions. These conditions range from the flow conditions present in the basic scour experiments. The focus for these experiments will be to study the behavior of the logs in a qualitative way, and thus determine boundary conditions for the application of logs and improvements for the experiments incorporating a scour protection made up of logs.

III.3.3 Cover of logs A.K.A Protected Scour

The final design of the experiments with a cover of logs was defined after conducting the single logs experiments. It was decided from the results of burial scour experiments that the Protected Scour experiments had to be subdivided into experiments with flow-parallel placed logs, and flow perpendicular placed logs.

Table 2; Test program

Name	Description	Water level [m]	Discharge [m^3/s]	Runtime [h]
Basic Scour 1	Gradual constriction induced scour	0.4	0,060	96
Basic Scour 2	Gradual constriction induced scour	0,4	0,060	96
Basic Scour 3	Gradual constriction induced scour	0,4	0,060	96
Burial Scour 1	Single log induced/amplified scour	0.4	0.040	24
Burial Scour 2	Single log induced/amplified scour	0.4	0.045	48
Burial Scour 3	Single log induced/amplified scour	0,4	0,050	72
Burial Scour 4	Single log induced/amplified scour	0,4	0,055	72
Burial Scour 5	Single log induced/amplified scour	0,4	0,060	96
Protected Scour A1	Contraction scour with a log carpet placed flow parallel in the area of maximum contraction	0,4	0,060	96
Protected Scour A2	Contraction scour with a log carpet placed flow parallel in the area of maximum contraction	0,4	0,060	96
Protected Scour A3	Contraction scour with a log carpet placed flow parallel in the area of maximum contraction	0,4	0,060	96
Protected Scour B1	Contraction scour with a log carpet placed flow perpendicular in the area of maximum contraction	0,4	0,060	96
Protected Scour B2	Contraction scour with a log carpet placed flow perpendicular in the area of maximum contraction	0,4	0,060	96
Protected Scour B3	Contraction scour with a log carpet placed flow perpendicular in the area of maximum contraction	0,4	0,060	96

IV Method

This section provides a brief overview, of how measured data will link theory to practice in this research study, and how measurements taken can be used to interpret, explain and predict the formation of scour in the laboratory set-up discussed in the previous section.

IV.1 Shields theory of sediment transport

As briefly mentioned in the preceding section, shields theory of sediment transport was used to estimate the flow velocity for sediment transport capacity. In order to verify these assumptions, discharge **(Q)** and the water level **(h)** must be monitored during the experiments. It was chosen to measure discharge with a so called flow meter, mounted on the return pipe, which eliminated uncertainty compared to flow velocity measurements. Water level heights are to be measured with a laser, using a reflective piece of paper floating on the surface. Alternatively, measuring tape can be used.

IV.2 Determination bed sediment transport

Sediment transport requires measurements of the bed at discrete time intervals. The application of a laser mounted in a boat with a transparent bottom will allow for the bed to be measured without having the problem of the laser passing through air which has a different diffraction coefficient and would therefor distort the data. In this specific application only a reference point under water is required. As the false bottom set-up in front of the experiment has an equal and known height of 20 [cm], this can be used to correct the measured data and produce relevant projections of the bed surface elevation and therefor scour depth **(d_s)**.

IV.3 Reynolds bed shear stresses & Relative fluctuation intensity

Determination of these properties is of importance to interpret scour development. These properties cannot be directly measured, but they can however be determined by measuring the flow properties close to the bed. These flow properties include average flow velocity (**($\overline{u}$), ($\overline{v}$)** & **($\overline{w}$)**) and the deviations from them (**($u`$)**, **($v`$)** & **($w`$)**). The relative fluctuation intensity will tell us the tendency of the flow to deviate from the mean. It is related to the tendency of individual grains being rocked loose from the bed due to alternating forces being acted upon them. It is however a non-dimensional expression of turbulence of a flow. The Reynolds bed shear stresses are however a measure of quantative measure of forces that does have a dimension and therefor is of even greater significance to the interpretation of turbulence and generation of scour.

IV.4 Hydraulic conditions

With the hydraulic conditions the roughness and consequently energy loss is meant. A depth **(d_s)** and water level height **(h_w)** measurement will be used to interpret the loss in energy due to the changes in bed friction/roughness.

IV.5 Measurement technique

As discussed earlier, measurement points for the vectrino profiler are appointed and visualized in Figure 13. Additionally the model is cut into separate sectors in order to more specifically address occurrences and their respective location, the division of sectors can be seen in Figure 14

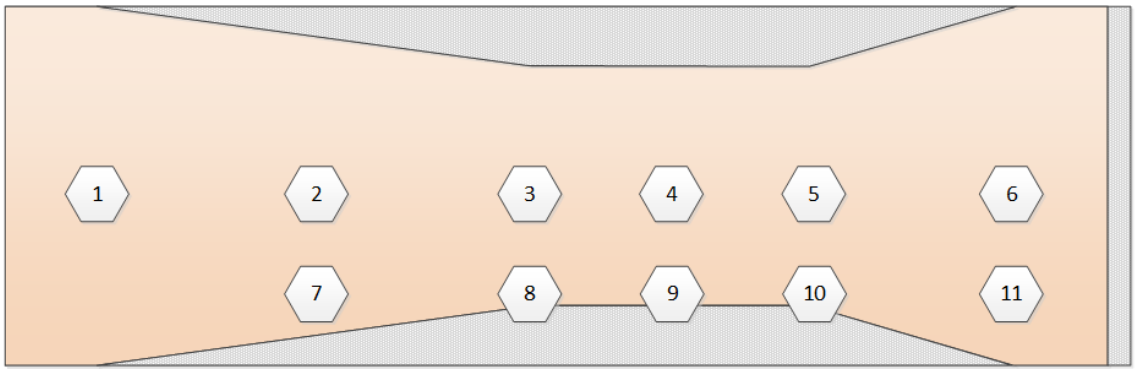

Figure 13; Measurement points

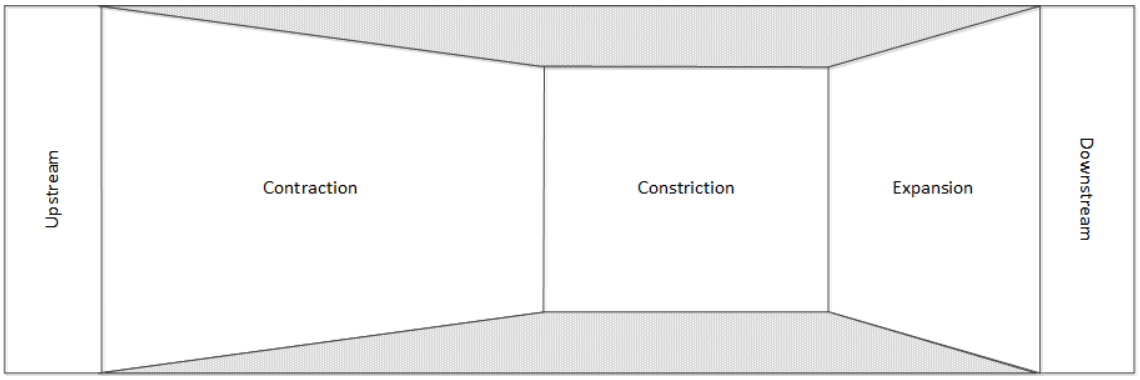

Figure 14; Sector division

1 Basic Scour Experiments

1.1 Results

From Figure 15-Figure 20, one can observe the development of scour over a period of 96 [h] (full sized versions available in Appendix BI, BII & BIII. Scour development was noticeably different for every run as is the maximum depth and total scoured volume. In accordance with calculations scour originates within the area of maximum constriction and consequently starts to destabilize the upstream slope, causing the scour to move upstream. This can be clearly seen in Figure 22 – Figure 26. Quantifiable results like the scoured volume and the maximum average scour depth can be seen in figure 11, figure 12 and table 2.

If for example, a look is taken at the development of scour for Basic Scour experiment I (Figure 21) , it is observable that that most of the occurring scour develops in the first 24 [h]. Right from the onset of flow it was visually observable that bed forms started to form halfway the contraction and were strongest in the fully constricted area. After the first 24 [h] this section also experiences the most scour and the largest scour depths. After 48 [h] it is observable that scour has amplified in the already afflicted constriction sector, but has now also started to eat away from the slope located the contraction sector. This eating away of the slope continues for the following 48 [h]. Scour seemingly has not arrived at equilibrium yet, as the scour accelerates in the last 24 [h]. The development of scour is similar for experiment number 2 and 3 although this acceleration is not observed so far into the experiments.

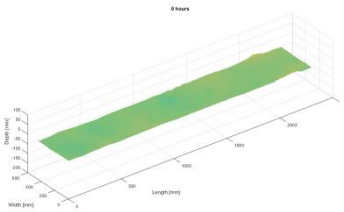

Figure 15; Bed Basic Scour 1 [0h]

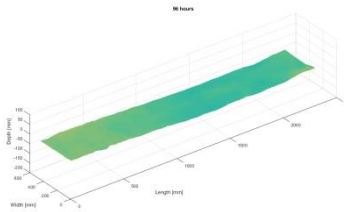

Figure 16; Bed Basic Scour 2 [0h]

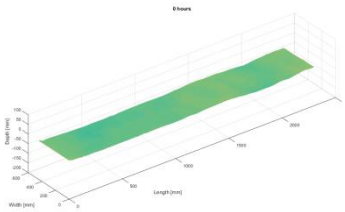

Figure 17; Bed Basic Scour 3 [0h]

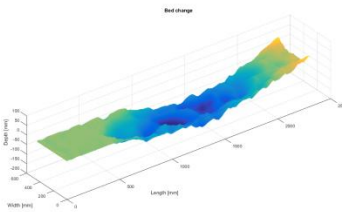

Figure 18; Bed Basic Scour 1 [96h]

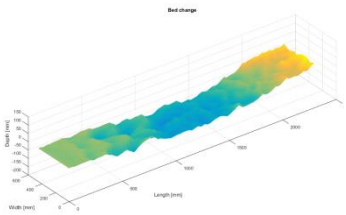

Figure 19; Bed Basic Scour 2 [96h]

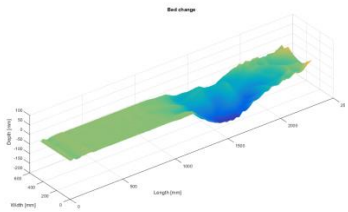

Figure 20; Bed Basic Scour 3 [96h]

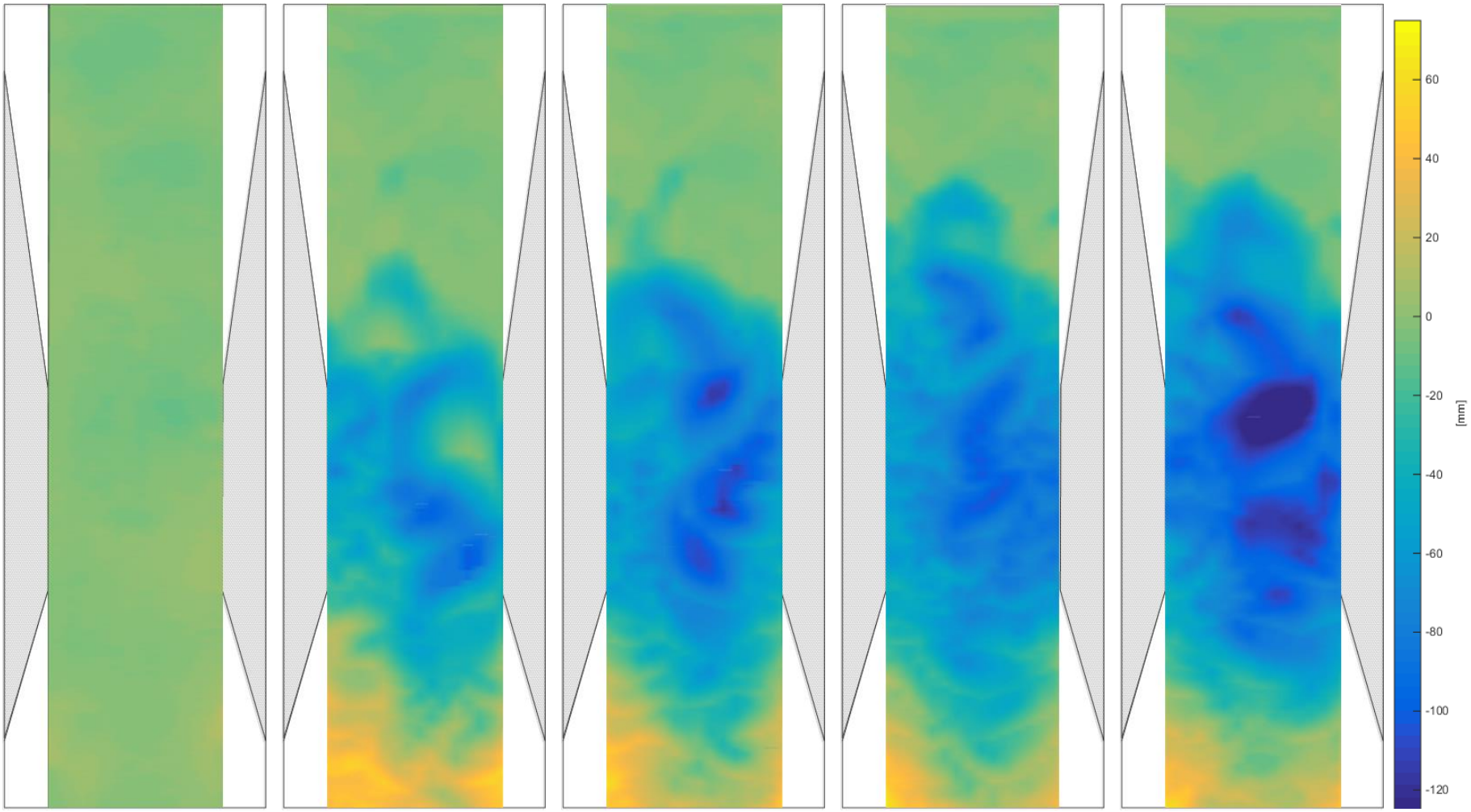

Figure 21; Progression of scour with intervals of 24 [h]

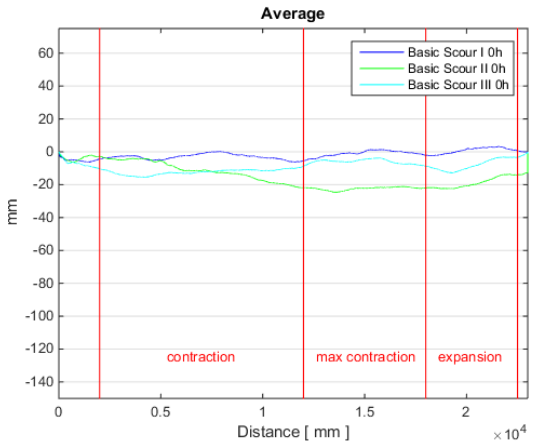

Figure 22; Average transects after 0[h]

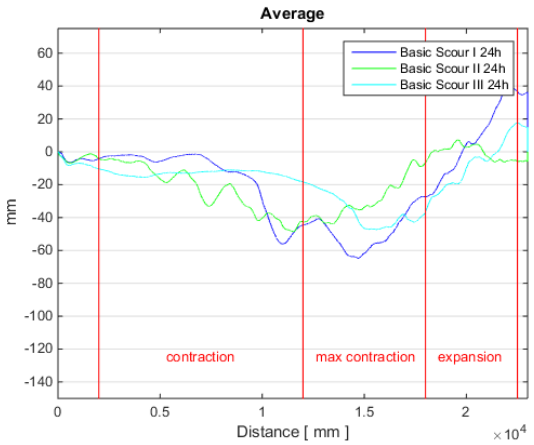

Figure 23; Average transects after 24[h]

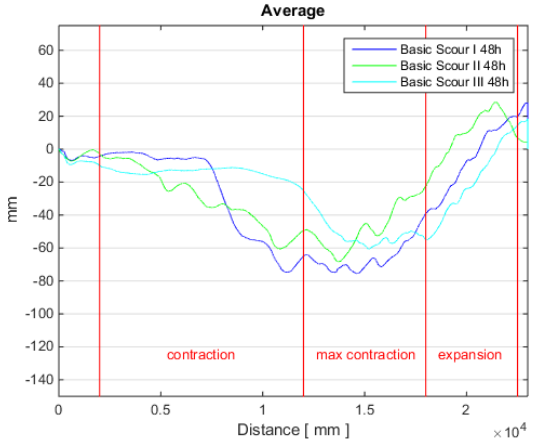

Figure 24; Average transects after 48[h]

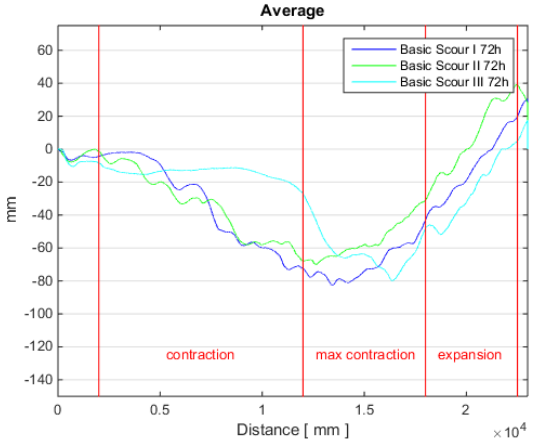

Figure 25; Average transects after 72[h]

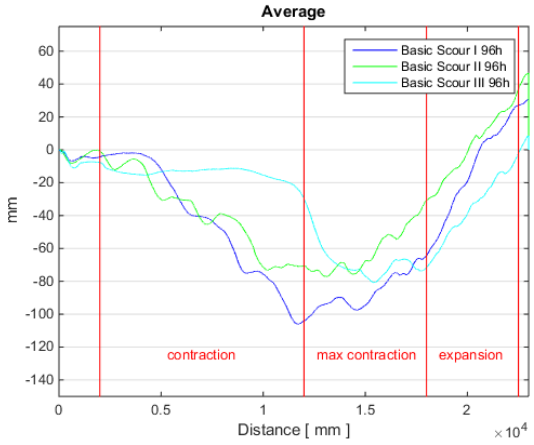

Figure 26; Average transects after 96 [h]

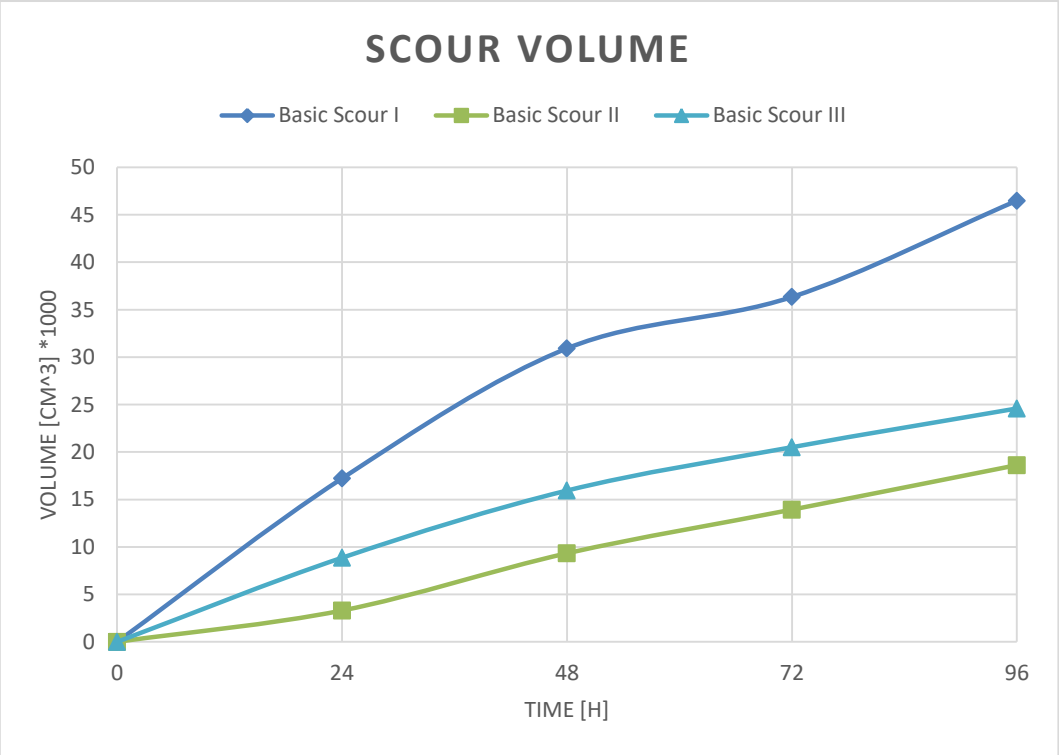

Figure 27; Absolute scoured quantities in [cm^3]

Table 3; Scour Quantity

Test number	Scour (24h) [cm^3]	Scour (48h) [cm^3]	Scour (72h) [cm^3]	Scour (96h) [cm^3]
1	17220	30920	36340	46490
2	3300	9330	13930	18620
3	8860	15940	20510	24590
Average	9793	18730	23593	29900

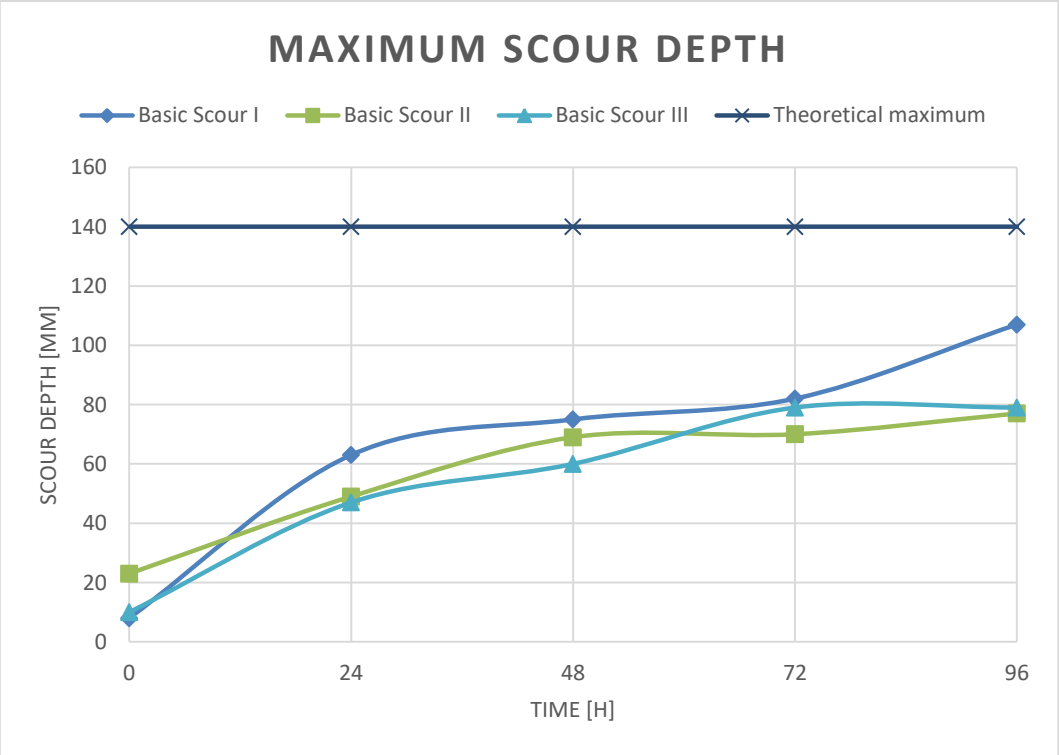

Figure 28; Maximum flume wide average Scour depth

1.2 Analysis

In this section quantitative and qualitative analysis will be made for the first three basic scour experiments. As can be observed in Figure 18, Figure 19Figure 20 (larger versions available in Appendix BI, BII & BIII), the Basic scour experiments showed very distinct scour patterns, and scour quantities. With the same boundary conditions of water level and discharge, the initial roughness and shape of the bed is seen as a possible cause for these differences. From Figure 22, it can be seen that the bed had a significantly higher initial level during the first basic scour experiment compared with the second and third basic scour experiments. If these initial differences are taken into account not by comparing scour to the starting level for each particular experiment, but to compare it to a relative elevation of 0 [cm] the quantities of Table 4 and graph of Figure 29 are obtained.

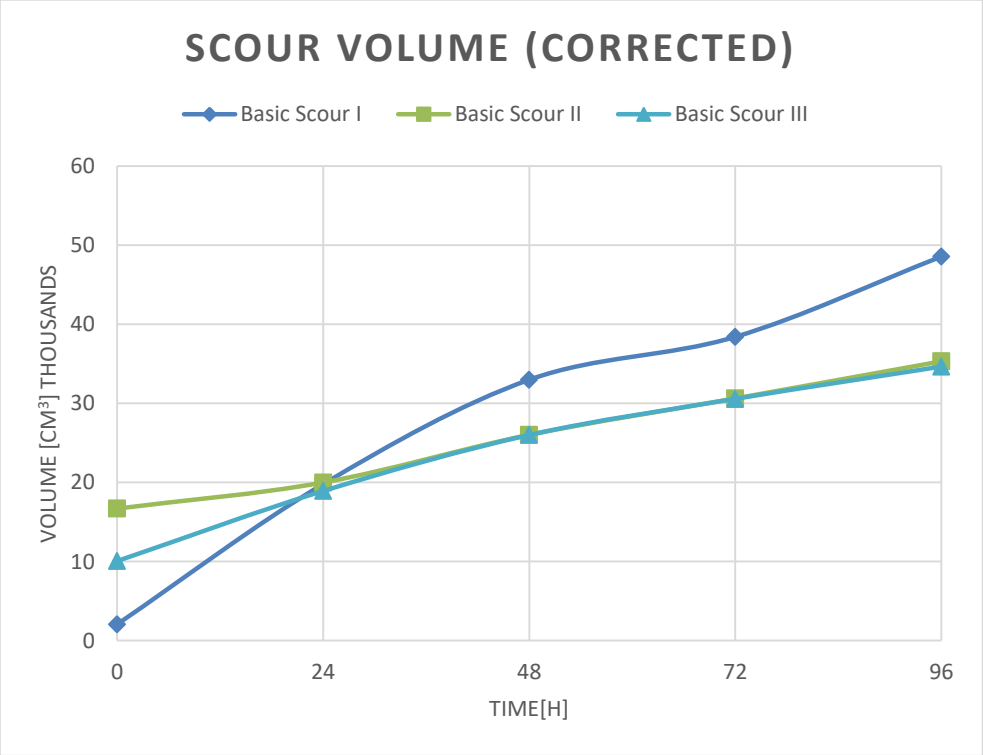

Figure 29; Scour volume corrected to reference elevation of 0

Table 4; Scour quantity corrected for initial bed level

Test number	Scour (24h) [cm³]	Scour (48h) [cm³]	Scour (72h) [cm³]	Scour (96h) [cm³]
1	19788	32988	38408	48558
2	19992	26022	30611	35312
3	18918	25998	30568	34648
Average	19566	28336	33199	39506

This graph shows a much narrower spread of scour volume, and even shows that the scour rate of Basic scour II and Basic Scour III are almost in line after the first 24 [h]. This approach to the scour volume is seen as more reliable, because differences in the initial bed can be interpreted as a scour experiment further along the path of scour development.

To further specify scour development, the model was divided into five sectors, namely: Upstream, Contraction, Constriction, Expansion and downstream (Figure 30). This, in combination with a measurement of the bed shear stresses, will be used to interpret the origin of scour development. As the bed shear stresses are not available for the first basic scour experiment, only the second and third will be investigated.

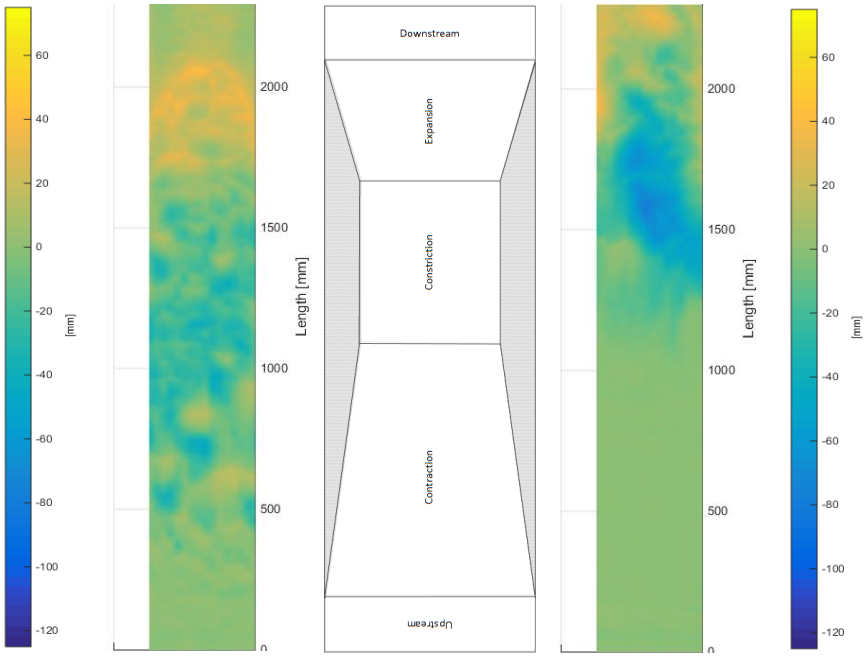

Figure 30; A comparison between bed changes for Basic Scour II & III during the first 24 [h]

As can be seen from Figure 30, the development of scour is distinctly different. Where in Basic Scour experiment 2 scour seems to develop over a longer stretch, Basic scour 3 shows a more intense scouring patch near the end of the area of maximum contraction. This would let to believe it should be observable that bed shear stresses are higher for Basic Scour experiment II at locations 2-3-4-7-8 while Basic Scour experiment III should show higher bed shear stresses at locations 5, 9 & 10. If the average of the bed shear stress measurements at 0 [h] and at 24 [h] is taken (Table 5) this hypothesis is confirmed.

Table 5; Average bed shear stress [n/m^2] 0-24 [h]

Location	1	2	3	4	5	6	7	8	9	10	11
BII	-0,068	-0,091	-0,211	-0,177	-0,207	-0,160	-0,127	-0,255	-0,129	-0,122	-0,213
BIII	-0,090	-0,063	-0,095	-0,107	-0,713	-0,365	-0,041	-0,045	-0,288	-0,379	-0,222

Additionally the bed shear stresses were used to predict scour rates according to Equation 8. The full results are depicted in Appendices BI, BII & BII but show that especially within the first 24 [h] the actual scour is in the same order of magnitude, although the bed shear stresses do seem to slightly over predict scour rates in the contraction, constriction and expansion sectors.

Upstream Sector

This sector shows for all three experiments very little changes with respect to the shape of the bed, as well as the scoured volume (Table 6 Upstream). As for this experiment an aim was made at clear water scour, the lack of scour in this sector is as expected

Contraction sector

The contraction sector has showed varied scour development. For experiments I & III the primary cause of scour is the collapse of the slope near the interface between the contraction and the constriction sectors, caused by scour in the constriction-sector. For experiment II the development of significant bed forms was however observed (Figure 22). A leading cause for this is most likely a clearly observable slope of the bed (Figure 22). This slope is approximately 2:100 which the shields parameter for the bed material, as grains easier roll downhill than uphill. This observation is supported by the development of bed forms originating from the beginning of the slope in basic Scour experiment II. The extra bed forms that develop in the first 24 [h] generated more turbulence (Appendix BII), this causes the scour formation pattern to develop as it does.

Constriction sector

The constriction is for all 3 experiments seen as the area where scour is strongest after 96 [h]. This is shown (Table 6 Constriction). Due to the sloping bed in Experiment II, it is only at the end of the experiment that the scour volume in the constriction overtakes the scoured volume in the contraction sector. Also observable is the point of maximum scour after 24 [h]. Which is approximately the same for experiment I & III, halfway the constriction sector. For the second basic Scour experiment this point is located more upstream at the interface between the contraction sector and the constriction-sector.

Expansion sector

This sector experiences mild scour throughout the experiments, but noticeable is a very strong deposition of scour for Basic Scour experiment II after the first 24 [h]. This can again be explained by the point of origin of scour for this particular experiment, which is located further upstream. Thus the particles haven't had enough time to leave the sector. After 24 [h] scour is of a similar magnitude for all experiments until the end of the experiments.

Downstream sector

The downstream sector shows alternating scour and accretion, total quantities are small compared to the other sectors (Table 6 Downstream). Observing the deposition in the first 24 [h], one can conclude that the scoured volume of experiment II indeed has a more upstream located origin, as this experiment shows far less deposition than the other two experiments.

Table 6; Absolute scour quantities per sector in [cm^3]

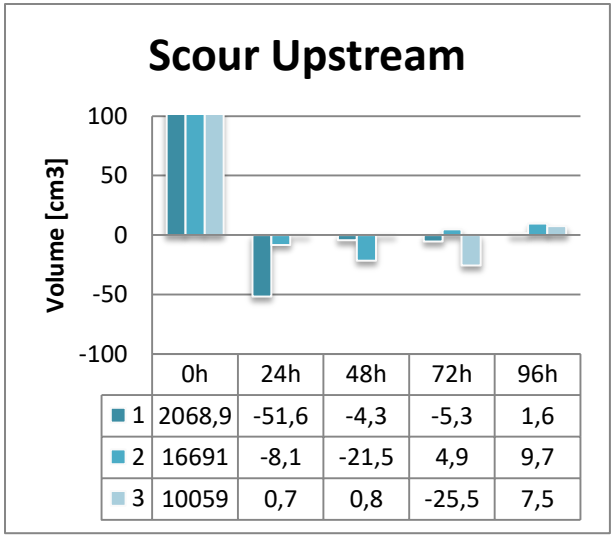

	0h	24h	48h	72h	96h
1	2068,9	-51,6	-4,3	-5,3	1,6
2	16691	-8,1	-21,5	4,9	9,7
3	10059	0,7	0,8	-25,5	7,5

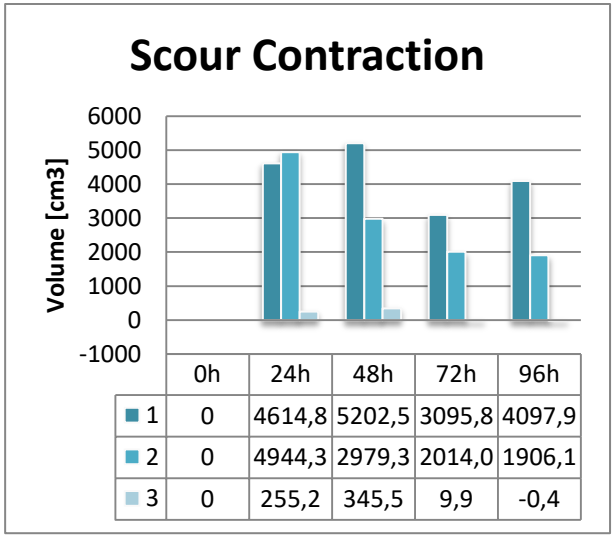

	0h	24h	48h	72h	96h
1	0	4614,8	5202,5	3095,8	4097,9
2	0	4944,3	2979,3	2014,0	1906,1
3	0	255,2	345,5	9,9	-0,4

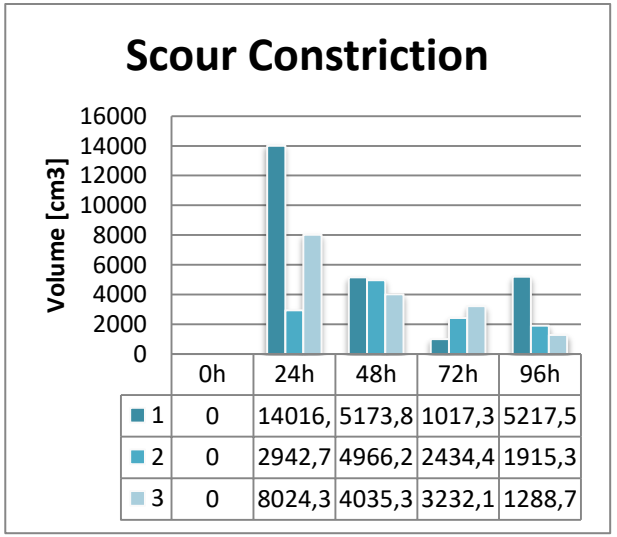

	0h	24h	48h	72h	96h
1	0	14016,	5173,8	1017,3	5217,5
2	0	2942,7	4966,2	2434,4	1915,3
3	0	8024,3	4035,3	3232,1	1288,7

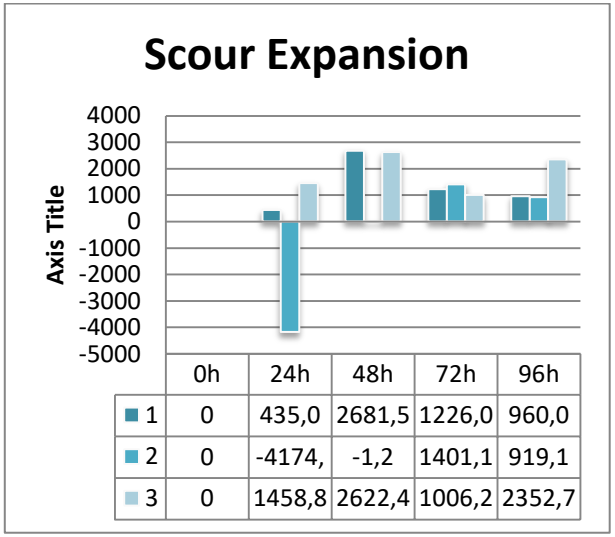

	0h	24h	48h	72h	96h
1	0	435,0	2681,5	1226,0	960,0
2	0	-4174,	-1,2	1401,1	919,1
3	0	1458,8	2622,4	1006,2	2352,7

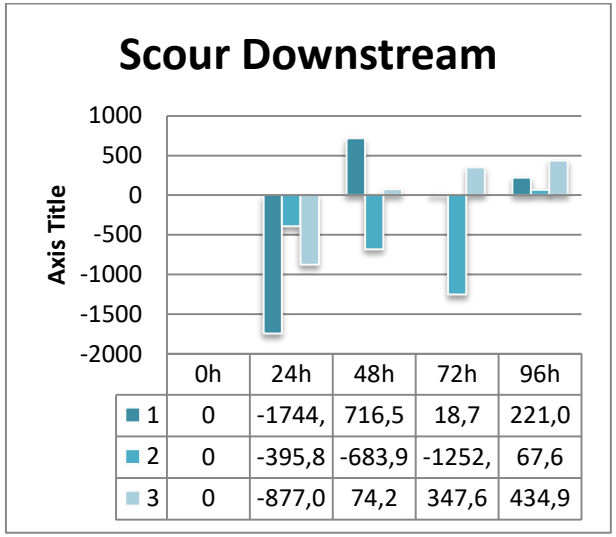

	0h	24h	48h	72h	96h
1	0	-1744,	716,5	18,7	221,0
2	0	-395,8	-683,9	-1252,	67,6
3	0	-877,0	74,2	347,6	434,9

1.3 Conclusion

From the basic scour experiments it was observed that the magnitude of scour was, after correction for initial bed differences, similar for all three experiments, but the scour formation pattern was distinctly different. As flow conditions were similar, differences in the initial bed were attributed as the primary cause for this phenomenon. In this light, it is advisable that additional experiments of this kind are conducted to obtain a statistical average and to validate the conclusion made with respect to the cause of the scour formation pattern.

The general picture however does show that progressive scour develops from the area of maximum contraction and moves upstream. Additionally, the concept of clear water scour appears to have been successful as the area upstream of the contraction shows little to no scour in all three experiments. Thus the primary focus for the log carpet experiments will be to monitor and prepare the initial bed, as flat as possible.

2 Burial Scour Experiments

In this section the results from the experiments with the placement of a single log placed in the area of maximum contraction will be discussed. In all five of the so called “burial scour experiments” the log was placed parallel to the flow (Figure 31)

Figure 31; Log placed parallel to flow

The goal of these experiments was to ascertain the morphological response caused by the log. Five experiments were conducted with increasing flow velocity (Table 7), and will be referred to as burial scour experiments.

Table 7; Burial scour test program

Name	Max. flow velocity [m/s]	Water level [m]	Discharge [m^3/s]	Runtime [h]
Single Log	0,200	0.4	0.040	24
Single Log	0,225	0.4	0.045	144
Single Log	0,250	0,4	0,050	72
Single Log	0,275	0,4	0,055	72
Single Log	0,300	0,4	0,060	96

2.1 Burial scour I

Burial scour I was conducted to ascertain the morphological effect the placement of a log would have on a previously non eroding bed. Discharge and water level were chosen such, that shields transport stage 3 was not violated. Thus frequent movement at some locations is expected, but on general no large transport rates should be present. This Velocity would correspond to the flow velocities that were reached upstream of the contracting section of the model in the Basic Scour experiments.

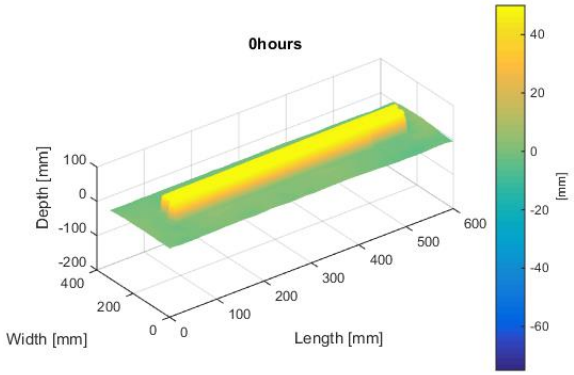

Figure 32; Bed scan [0h]

After placement of the log on the bed a scan was made (Figure 32) and a video camera was mounted to capture the scour formation progress. After 24 [h] the experiment was halted due to the limited influence the log had made on the surface.

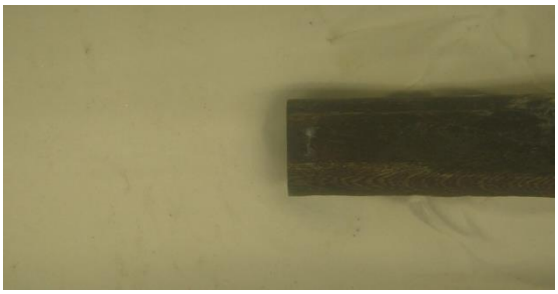

Figure 33; Bed morphology after 10[h]

2.2 Burial scour II

Burial scour II was conducted at a higher flow velocity that should not violate shields parameter 4, thus frequent movement at many locations is expected. As with burial scour I, a scan was made of the bed at initiation of flow (Figure 34). This time the scan was widened to visualize a larger part of the bed around the log.

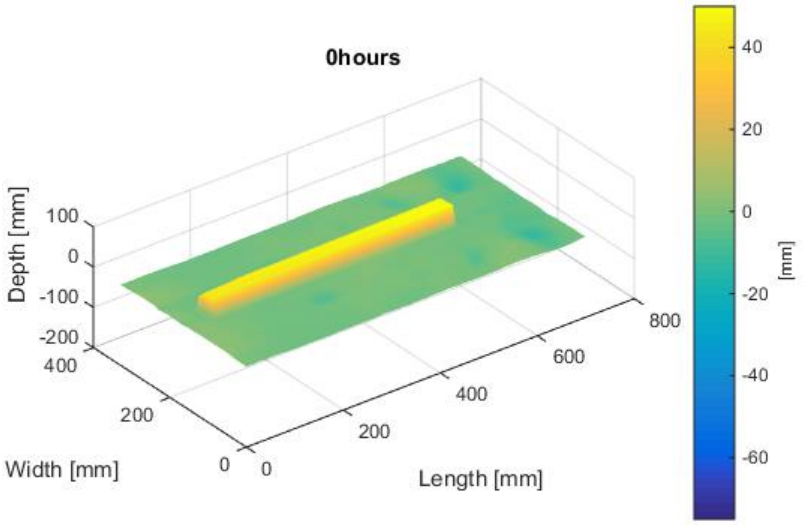

Figure 34; Burial Scour II: bed scan 0[h]

The bed showed some minor indentures but on average the bed was relatively flat. Shortly after initiation of flow (15 [min]) bed forms developed around the log in the shape of a horseshoe (Figure 35). During the next 10 hours this scour pattern would increase in magnitude to reach Figure 36 (Full scour development in appendix CII)

Figure 35; Burial scour II: 15 [min] after initiation of flow

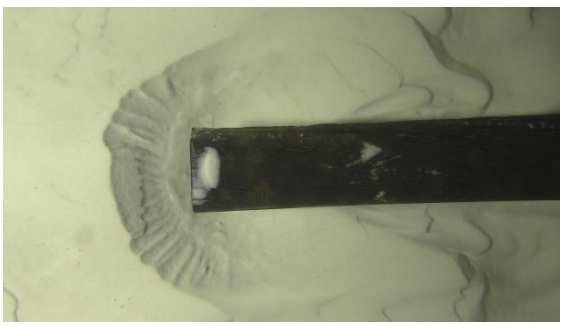

Figure 36; Burial scour II: 10 [h] after initiation of flow

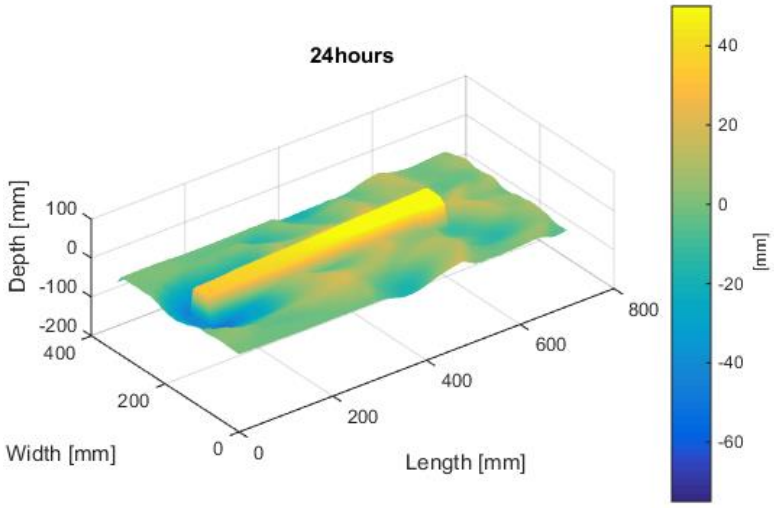

Figure 37; Burial Scour II: bed scan 24 [h]

After 24 hours (Figure 37) it was visible that the log had generated a significant scour hole at its front face and it consequently started to tilt towards this scour hole. Scour development was further monitored by measuring the bed every 24 hours. This was continued for a total of 144 hours, after which the experiment was ended. During this time period the log tilted and shifted further, causing the face to drop below the initial bed level (Figure 38). Scour progression slowed significantly and to favored one side of the log more heavily. On the downstream end of the log scour was observed, but this was relatively small compared to scour at the front face

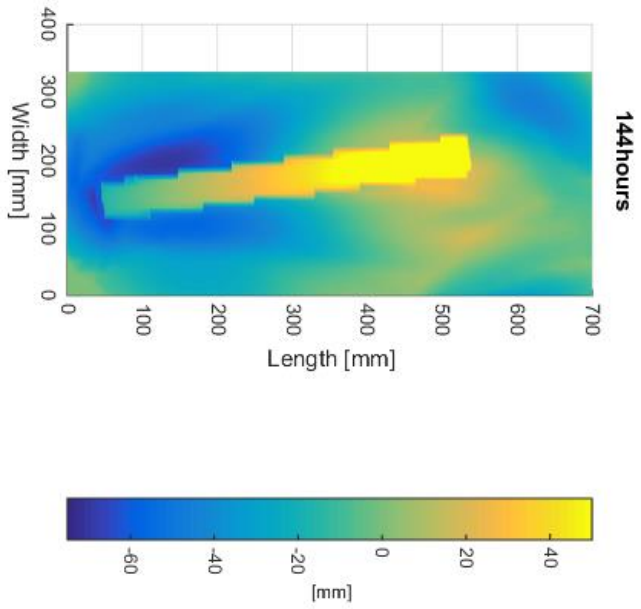

Figure 38; Burial Scour II: bed scan 144 [h]

2.3 Burial scour III

The third experiment was executed with an even higher discharge, now able to violate the fifth shields parameter. Thus frequent movement at all locations was expected. A scan was made of the bed at initiation of flow.

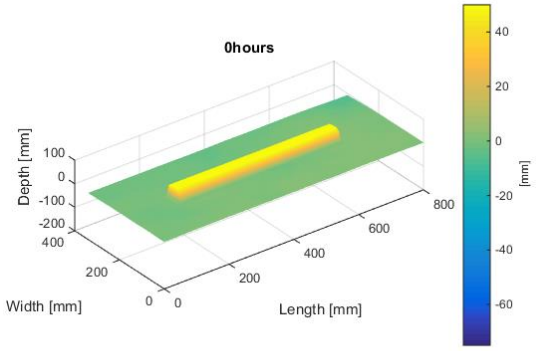

Figure 39; Burial Scour III: Bed scan 0[h]

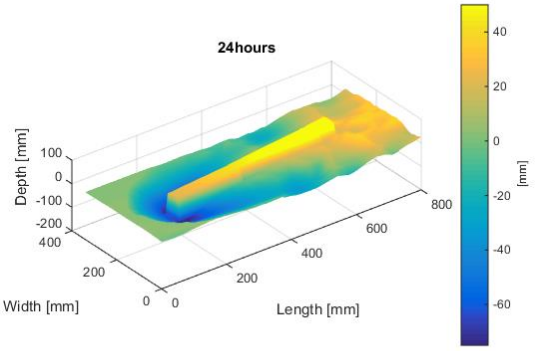

Figure 40; Burial Scour III: Bed scan 24[h]

This time the scan was widened even further to visualize a larger part of the upstream bed around the log. Again the log was placed on a relatively flat bed. After 24 hours scour at the upstream face of the log reached up to 7 [cm] and the log had again started to tilt and shift towards the scour hole.

After 72 hours (Figure 41) the log had now almost completely buried its way through the bed and was now almost completely below the initial bed level. The log had again shown to turn towards one side, causing more scour on the side facing the flow. Scour progression was slow at this point, thus the experiment was ended.

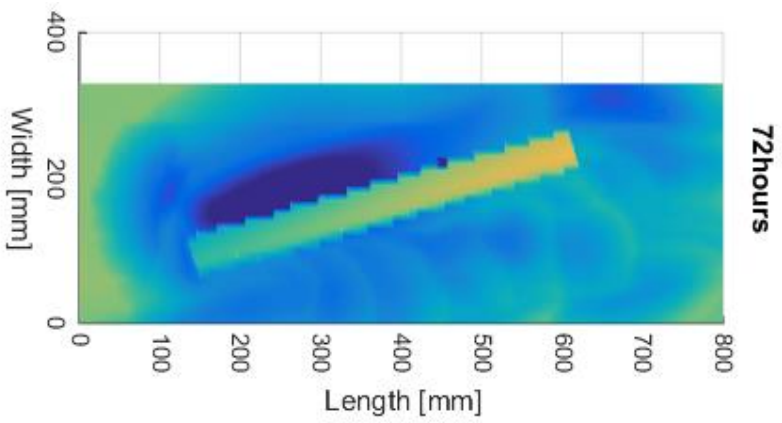

Figure 41; Burial Scour III: Bed scan 72[h]

2.4 Burial scour IV

The fourth experiment was executed with an average velocity of 27,5 [cm/s], now able to violate the sixth shields parameter. Thus continuous movement at all locations is to be expected. As before, a scan was made of the bed at initiation of flow (Figure 42).

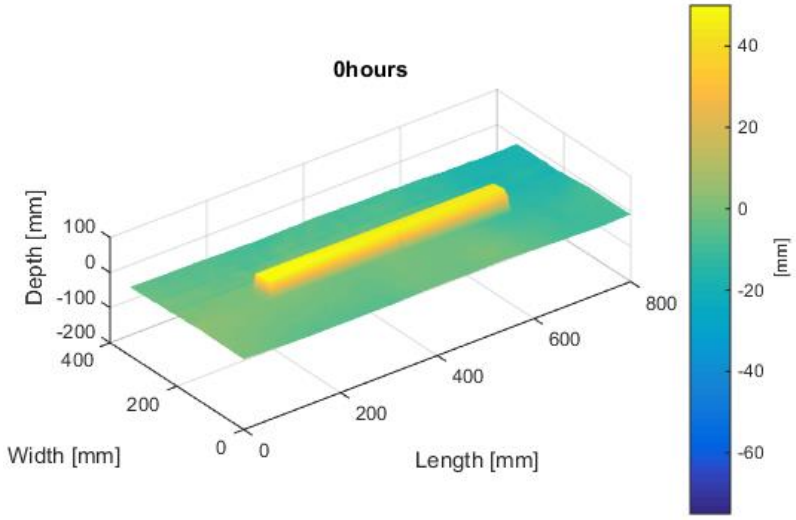

Figure 42; Burial Scour IV: Bed scan 0 [h]

The traditional horseshoe shaped scouring hole that was observed in previous experiments was not observed in this experiment. Instead, due to feeding of sediment from upstream areas the horse shape collapsed. After two and a half hours of steady flow the scour did develop at the upstream face of the log, but the pattern was now disturbed (Figure 43).

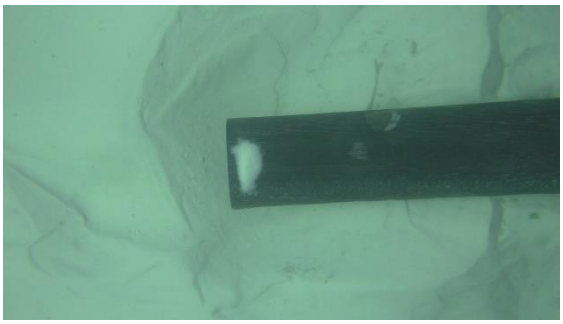

Figure 43; Burial Scour IV: Bed image after 2h30m

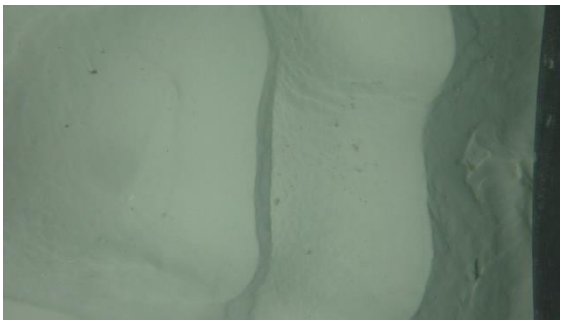

Figure 44; Burial Scour IV: Bed image after 16h

From video imagery it was observed that the log apparently turned about 90 degrees within 15 minutes six hours after initiation of flow and had now assumed a position perpendicular to the governing flow direction. This led to the development of a trench upstream of the log. 48 hours into the experiment (Figure 45) the bed upstream of the log started to smooth out and accrete to the log.

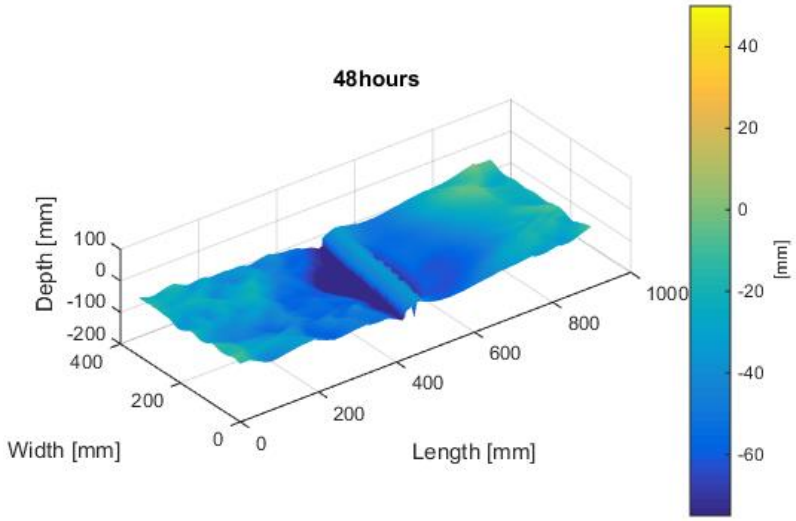

Figure 45; Burial Scour IV: Bed scan 48 [h]

After 72 hours the downstream side of the log was now fully embedded into the bed (Figure 46). This, together with limited progression between 48[h] & 72[h], prompted the end of the fourth burial scour experiment.

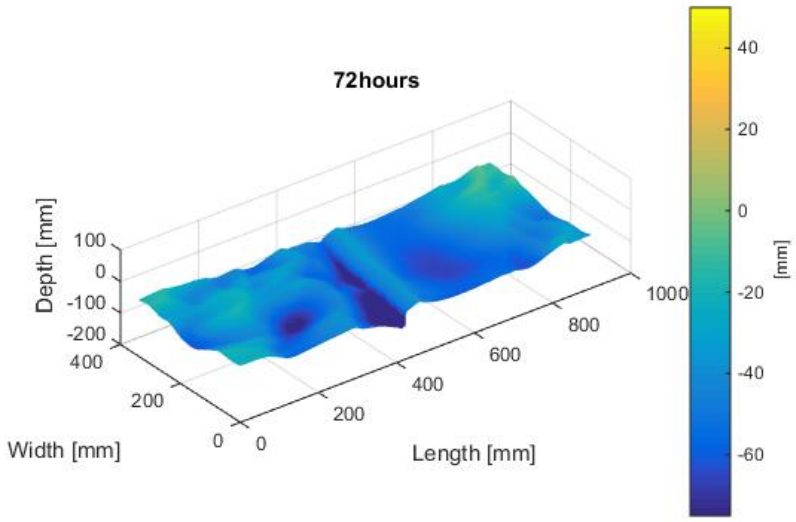

Figure 46; Burial Scour IV: Bed scan 72 [h]

2.5 Burial scour V

The fifth and final experiment was executed with the same flow conditions as the basic scour experiments (namely 40 [cm] water depth and 60 [dm^3/s] discharge). As before, a scan was made of the bed at initiation of flow (Figure 47).

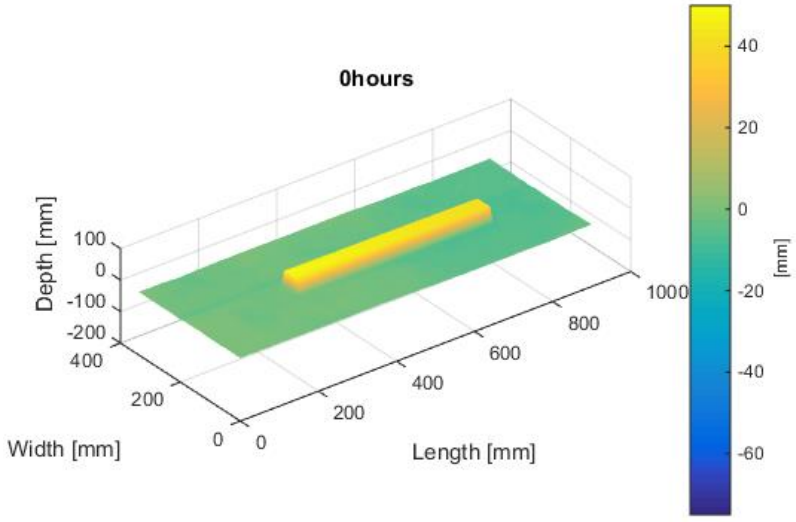

Figure 47; Burial Scour V: Bed scan 0[h]

The log again started to turn, this time after 5 hours of flow. Similar as to Burial scour experiment IV, the log started to accrete on the downstream side, until the top of the log was connected to the bed, and the bed had thus formed a sort of natural silt (Figure 48). It was decided to continue the experiment for the total duration of 96 hours, to allow for comparison with the basic scour experiments.

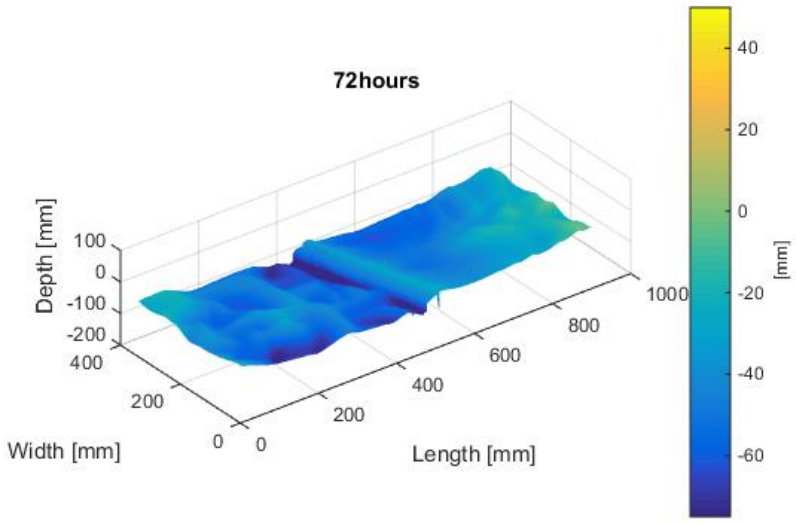

Figure 48; Burial Scour V: Bed scan 72[h]

After 96 hours, downstream of the log the bed was still relatively smooth, but the area around the log had started to erode again, and the bed level on the downstream end did no longer form a connection with the top of the log (Figure 49). The log now started to show signs of what might be interpreted as a pipeline scour mechanism, scour holes expanding horizontally towards the center originating from the side faces of the logs (Figure 49) (Mutlu Sumer and Fredsøe 2005).

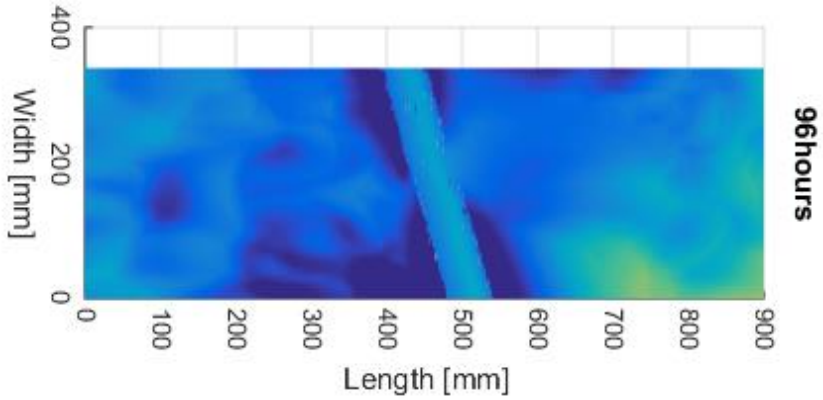

Figure 49; Burial Scour V: Bed scan 96 [h] top view

After this point (96[h]) the experiment was stopped. A scan of the global morphology was made (Figure 50). This showed a global scour pattern similar to basic scour experiments I & II. More detailed imagery of this can be found in Appendix CV.

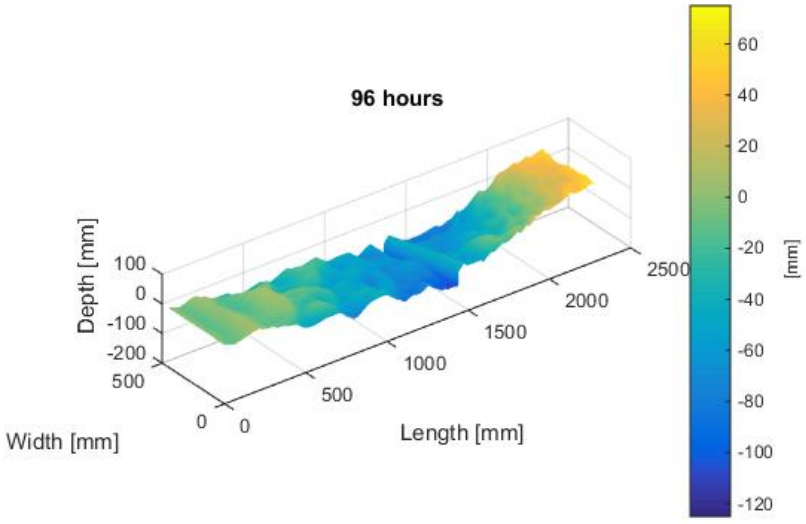

Figure 50; Burial Scour V: Global morphology after 96 [h]

2.6 Conclusion

From the Burial scour experiments it was observed that small changes in the average flow velocity had a very large impact on the bed morphology. When naturally movement of the bed is limited, the bed will start to develop a horseshoe shaped scouring hole underneath the front face of the log. The magnitude of this scouring hole increases significantly with small changes in the velocity. When flow velocities reach speeds that would cause the bed to scour rapidly on its own, this typical horseshoe shaped scouring hole is disturbed and over some time, the log will tend to turn until it has assumed a perpendicular position with respect to the governing flow direction. At this point the bed downstream of the log appears to erode less quickly then its upstream counterpart until it starts to scour from the edges towards the center of the log. Due to the tendency of the log to turn perpendicular and then stabilize the bed downstream for a given period of time, the placement of a carpet of logs also placed perpendicular to the flow might produce better scour protection than placement of the logs parallel to the flow. For this reason exploring both possibilities is advised for the remainder of the experiments.

3 Protected Scour Experiments

3.1 General observations

During the experiments two basic mechanisms were observed. The logs placed flow parallel followed a so called cantilever mechanism, while logs placed perpendicular to the governing flow direction followed a staircase mechanism Figure 51. Both mechanisms go through four stages of development, these are discussed henceforth.

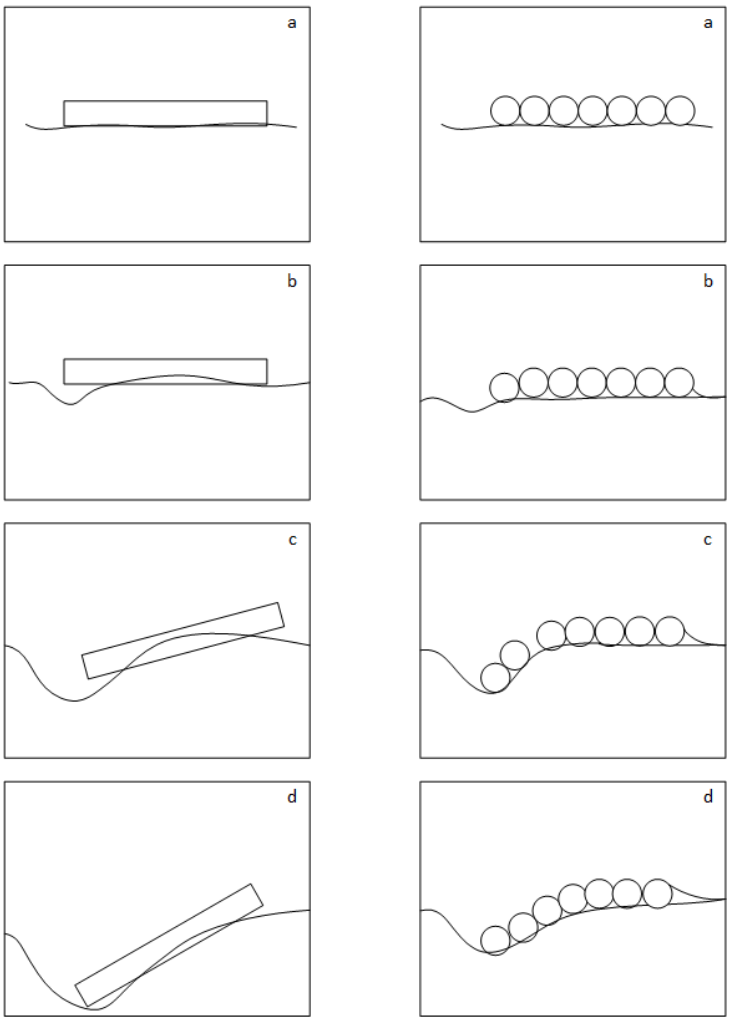

Figure 51; Log carpet mechanisms for flow parallel placed logs (left) and flow perpendicular placed logs (right)

3.1.1 Cantilever

This mechanism is applicable for logs placed parallel to flow and observable in Figure 51 (a-d left).

a) The first stage of the cantilever mechanism occurs at the initiation of flow, the logs are located on a level bed. No scour has occurred yet. Immediately from the start bed load transport is observable at the upstream face of the log layer.

b) The second stage of the cantilever mechanism occurs within the first hours after initiation of flow. Several shallow scour holes form underneath each of the upstream faces of the logs. Scoured material is transported by dunes in between the logs and at this point scour resembles to some degree pier scour.

c) The third stage generally occurs within the first 24 [h], the scour underneath the front faces has formed a single concentrated scour hole. One or more of the logs the logs have started to tilt towards the scour hole. This causes their faces to drop and further intensification of scour occurs. Consequently the downstream end of the logs is raised above their initial level.

d) The fourth and final stage is a continuous stage where scour keeps growing over the course of the next 48-72 [h]. The logs are now completely below the initial bed level. Scour at the front face has reached a maximum depth, but scour underneath the logs continuous to sink the logs further into the bed.

3.1.2 Staircase

This mechanism is applicable for logs placed perpendicular to flow and is observable in Figure 51 (a-d right).

a) The first stage of the staircase mechanism occurs at the initiation of flow, the logs are located on a level bed. No scour has occurred yet. Immediately from the start scour is observable at the edges of the most upstream located log.

b) The second stage of the staircase mechanism shows the development of a near uniform trench in front of the most upstream located log. The growth pattern resembles traditional pipeline scour pattern where scour holes from the sides of the log move towards the center. The log has not shown much, if any, movement at this time

c) The third stage of the staircase mechanism shows the most upstream located log has rolled into the scour hole it developed at the front face. This exposes bed underneath the second log to the flow, causing it to rapidly follow the first log and rolling towards the scour hole.

d) The fourth stage usually follows with a third or fourth log rolling towards already displaced logs, forming a staircase of logs and no longer exposing any bed material underneath the logs. This results in a significant reduction of scour rates underneath the logs.

3.2 Results

The results of the experiments incorporating a cover of logs are discussed in this section. A division between logs placed parallel to the governing flow direction (A-series) and logs placed perpendicular to the governing flow direction (B-series). Figure 52, Figure 54 & Figure 56 portray the results of the A-series experiments after a runtime of 96 [h]. Figure 53, Figure 55 & Figure 57 portray the same for the B-series experiments. Observable from these figures is already distinct behavior of the logs that was discussed in the preceding section. The results and analyses will therefore be presented separately to the reader.

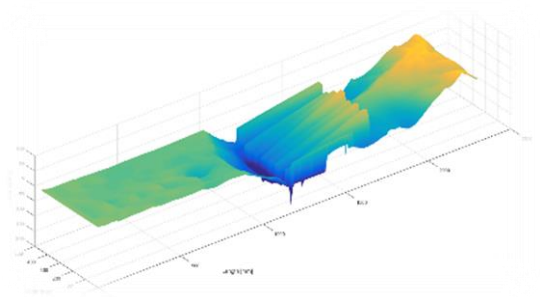

Figure 52; Protected Scour A1 96 [h]

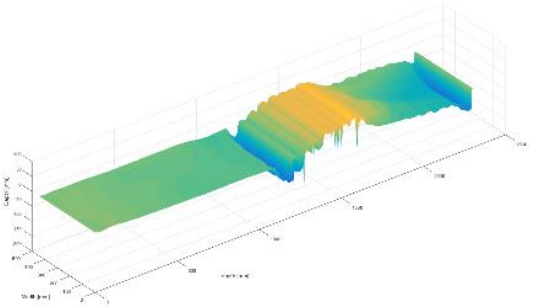

Figure 53; Protected Scour B1 96 [h]

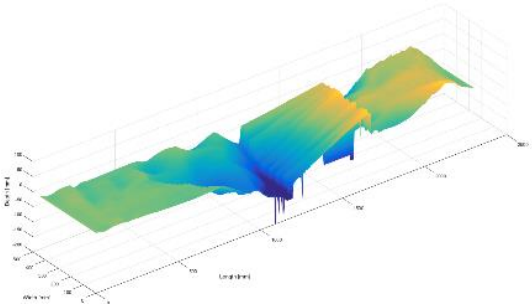

Figure 54; Protected Scour A2 96 [h]

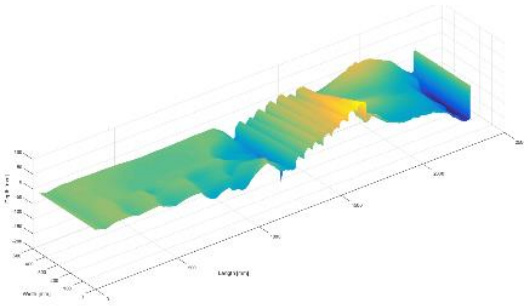

Figure 55; Protected Scour B2 96 [h]

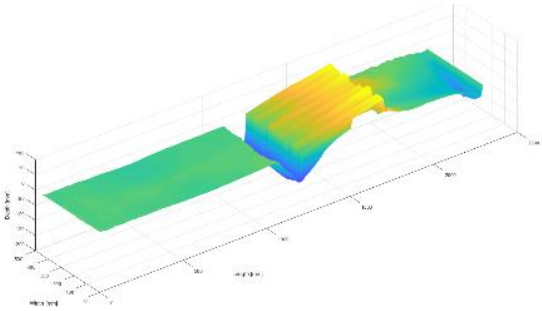

Figure 56; Protected Scour A3 96 [h]

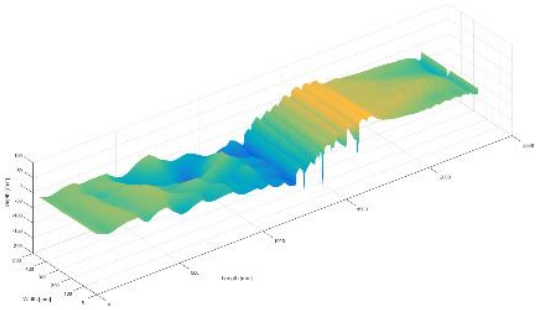

Figure 57; Protected Scour B3 96 [h]

3.2.2 Protected Scour Experiments – A series – Flow parallel

The results of the experiments with flow parallel show to develop scour quantities as stated in Figure 58 & Table 8. Note that these values are absolute scour quantities, and results from integrating the measured differences of the bed in between two measurements in time. Figure 59 shows that the maximum measured width average scour depth for these experiments ranged between 95-125 [mm] after 96 [h]. The maximum scour depths where for all three cases measured at the upstream face of the logs.

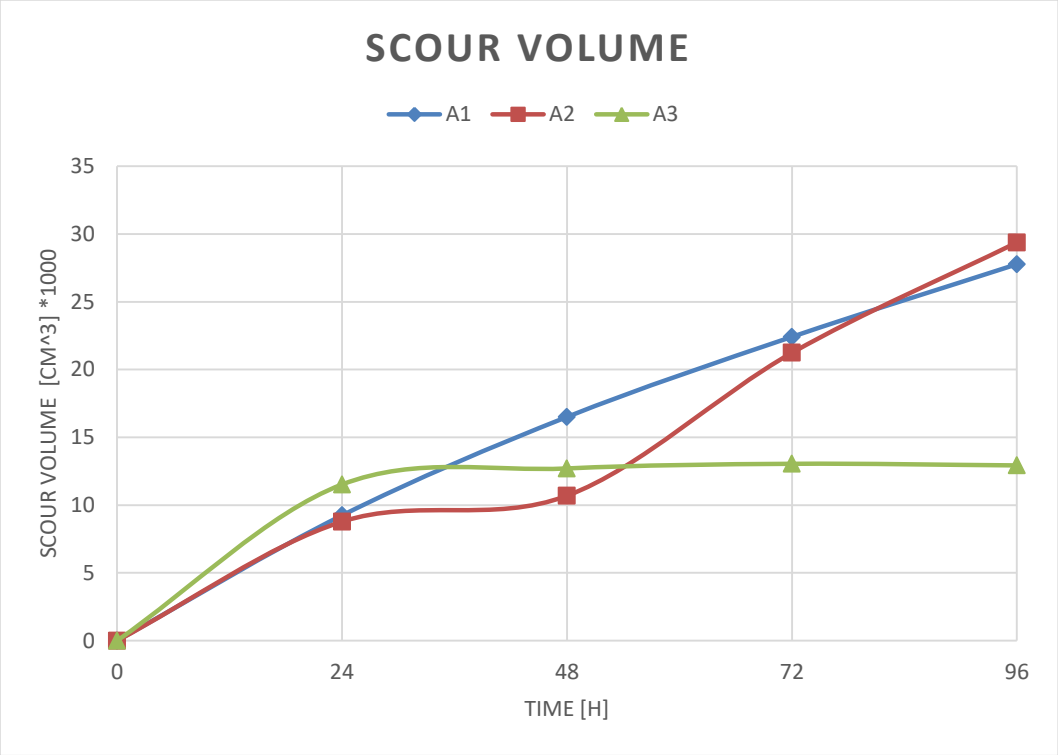

Figure 58; Absolute scoured volume for A-series (flow parallel)

Table 8; Absolute scoured volume for A-series (flow parallel)

Test number	Scour (24h) [cm³]	Scour (48h) [cm³]	Scour (72h) [cm³]	Scour (96h) [cm³]
1	2673,20	9934,00	15843,69	21199,19
2	1512,84	3420,71	13966,71	22104,51
3	3234,97	4418,62	4761,23	4888,0
Average	2473,67	5924,44	11523,87	15981,78

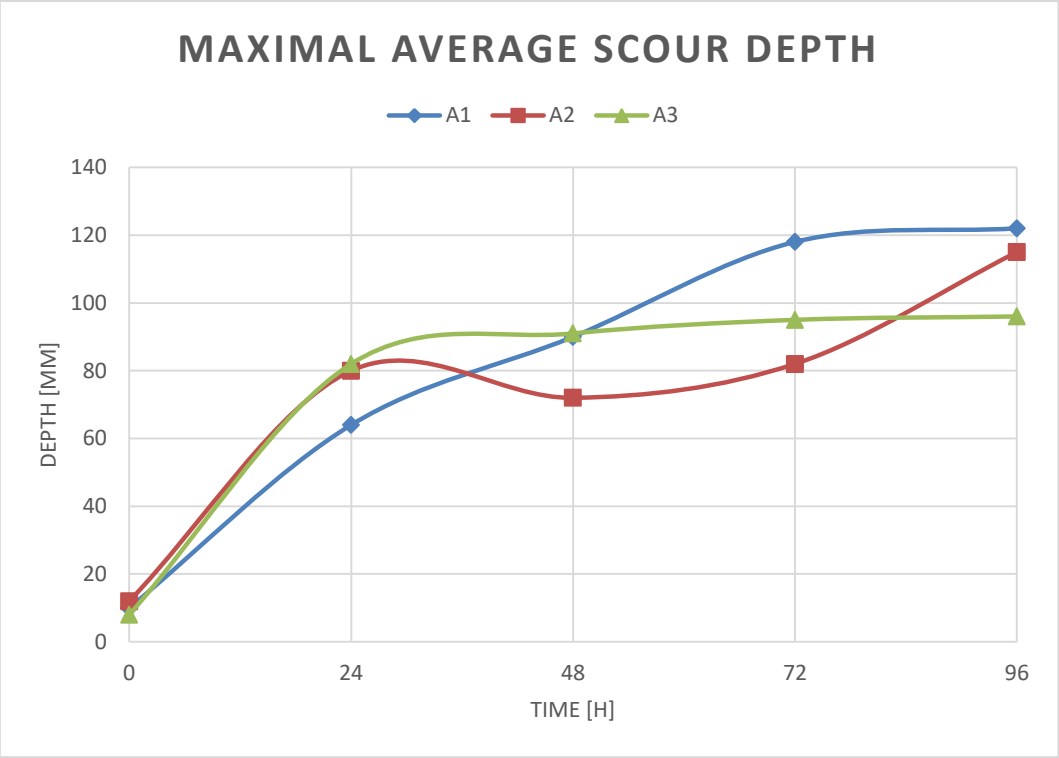

Figure 59; Maximum cross section averaged scour depth for A-series (flow parallel) in [mm]

For arguments sake the results of protection scour A1 are henceforth discussed. A complete report for every experiment can be found in Appendix D1, DII & DIII. From the onset of flow, the log layer acts like a vertical step and consequently flow behind the logs can be described as severely disturbed, as can be seen in flow profiles and projections of the fluctuation intensity at locations downstream of the log layer (Figure 60 - Figure 65). Interesting to note is that in contrast to a traditional vertical step, near bed velocities are directed both downstream and upstream, depending on the exact location.

A measurement of the bed shear stresses show that from the start, locations primarily downstream of the logs (5-10-11) face heavy attack. Values above a magnitude of 0,16 [n/m^2] are associated with scour following the results basic scour experiments, and are thus made red. Locations 4 & 9 are located and measured on top of the log layer, and thus do not represent the actual values near the bed.

Table 9; Bed shear stress at onset of motion [n/m^2] 0 [h] following the Reynolds method specified per location

	1	2	3	4	5	6	7	8	9	10	11
A1	-0,052	-0,004	-0,047	-0,118	-0,307	-0,054	-0,009	-0,027	-0,062	-0,023	-0,288
A2	-0,059	-0,006	-0,101	-0,337	-0,314	-0,117	-0,063	-0,049	-0,231	-0,193	-0,229
A3	-0,065	-0,044	-0,071	-0,150	-0,188	-0,123	-0,062	-0,048	-0,071	-0,309	-0,045

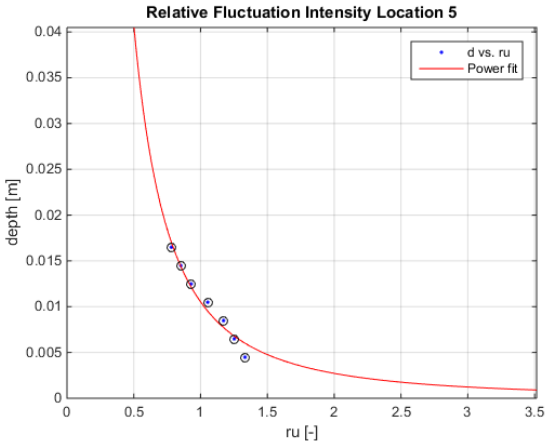

Figure 60; Calculated RFU in the primary flow direction, with depth as distance from the bed for location 5 experiment A-1

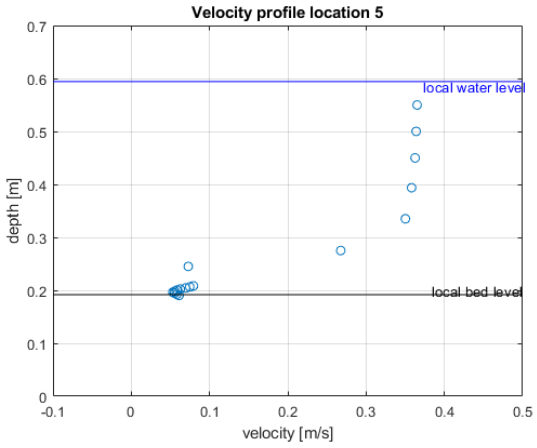

Figure 61; Velocity Profile for location 5 experiment A-1 with depth relative to the bottom of the flume.

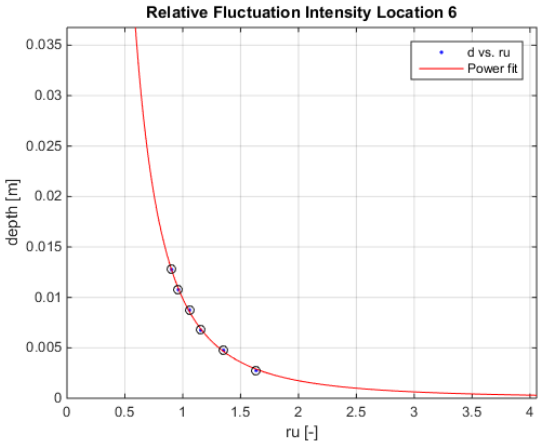

Figure 62; Calculated RFU in the primary flow direction, with depth as distance from the bed for location 5 experiment A-1

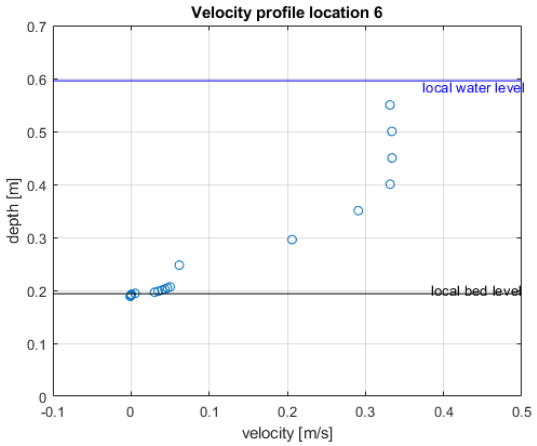

Figure 63; Velocity Profile for location 6 experiment A-1 with depth relative to the bottom of the flume.

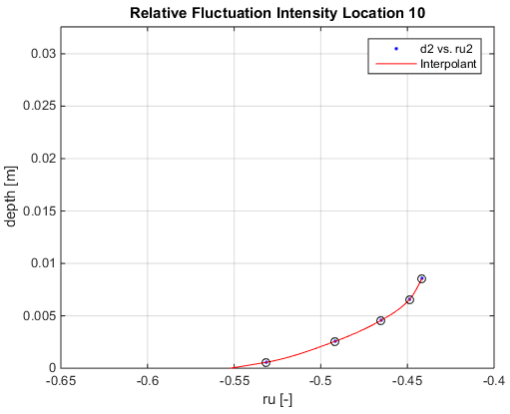

Figure 64; Calculated RFU in the primary flow direction, with depth as distance from the bed for location 10 experiment A-1

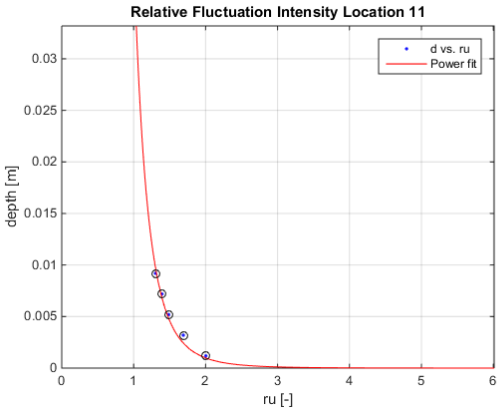

Figure 65; Calculated RFU in the primary flow direction, with depth as distance from the bed for location 11 experiment A-1

Figure 66 - Figure 70 show the cantilever mechanism that was discussed in section 3.1.1 This mechanism has occurred for all three experiments. Within the first 24 [h] the very steep scour hole that has developed underneath the upstream face of the log layer causes either one or more logs to tilt inwards. The downstream face of the logs consequently raise, causing a proportionally larger part of the cross-section to be obstructed by the logs.

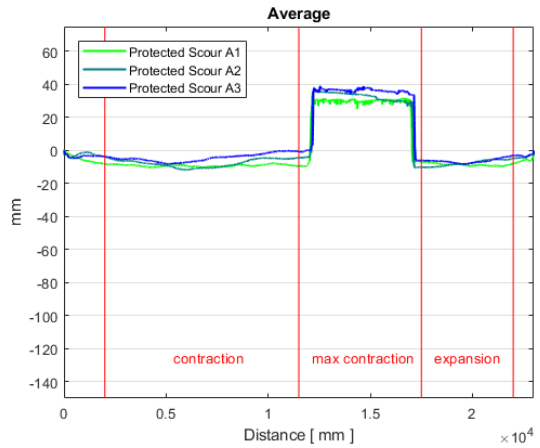

Figure 66; Average transects after 0[h]

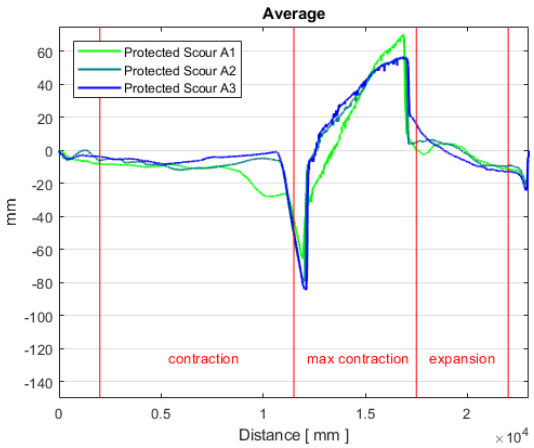

Figure 67; Average transects after 24[h]

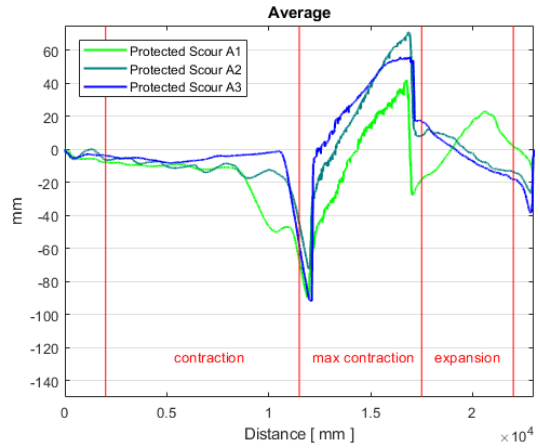

Figure 68; Average transects after 48[h]

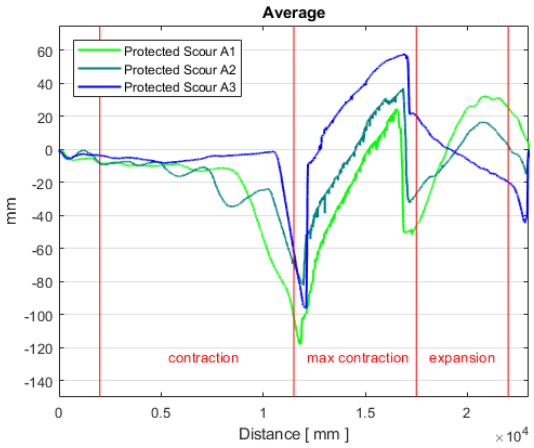

Figure 69; Average transects after 72[h]

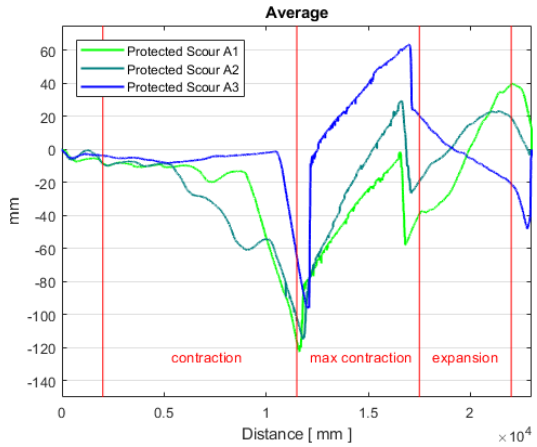

Figure 70; Average transects after 96[h]

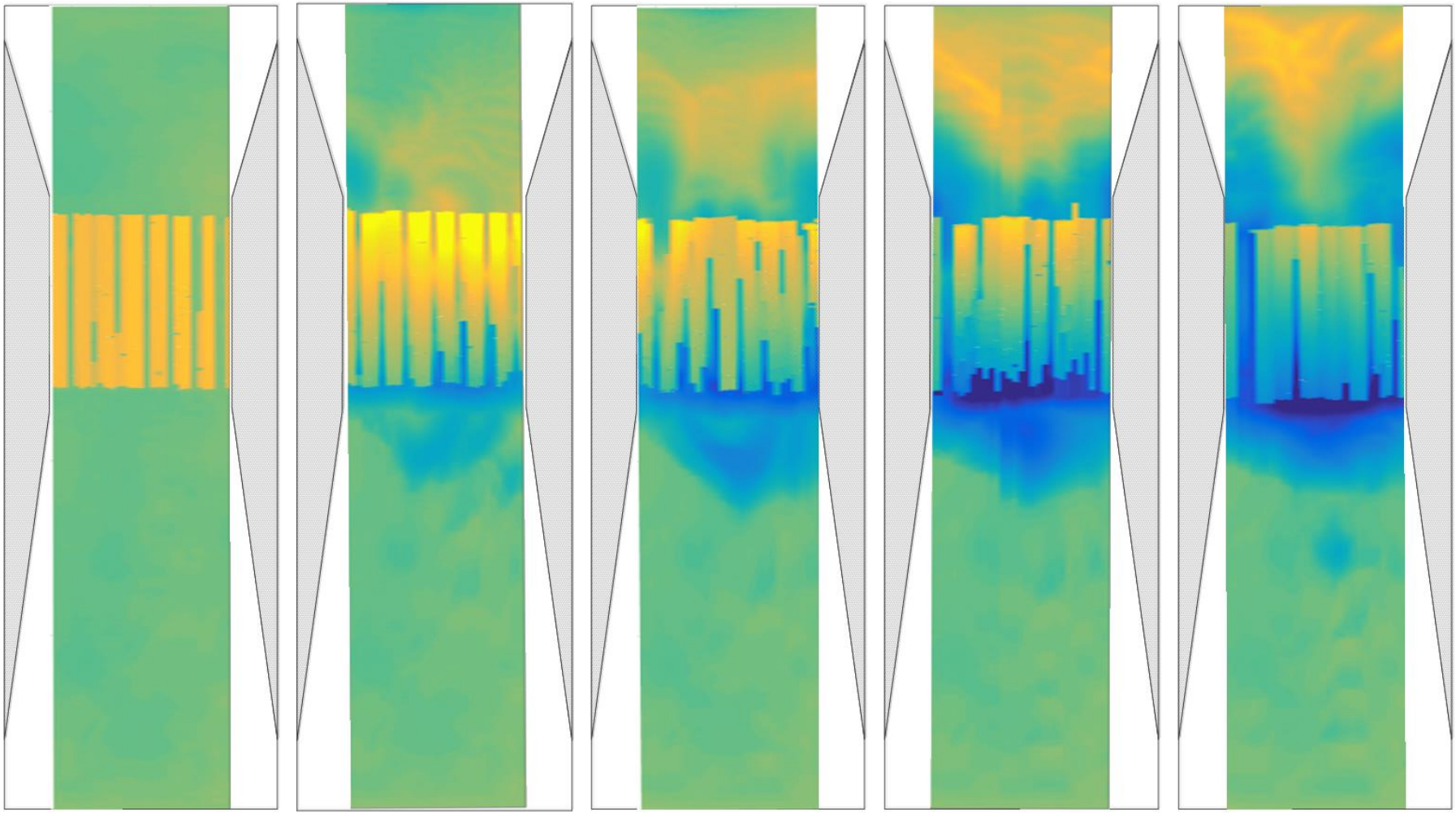

Figure 71; Progression of scour for flow parallel placed logs with 24 [h] intervals

3.2.3 Protected Scour Experiments – B series – Flow perpendicular

The results of the experiments with flow perpendicular logs how to develop scour quantities as stated in Figure 72 & Table 10. Note that these values are absolute scour quantities, and results from integrating the measured differences of the bed in between to measurements in time. Figure 73 shows that the maximum measured width average scour depth for these experiments ranged between 85-125 [mm] after 96 [h]. The maximum scour depths was in two cases measured upstream of the logs, for one case this depth was measured in the section near the downstream end. If only the scour depth the constriction-sector is taken into account the maximum measured width averaged scour depths do not exceed 85 [mm]

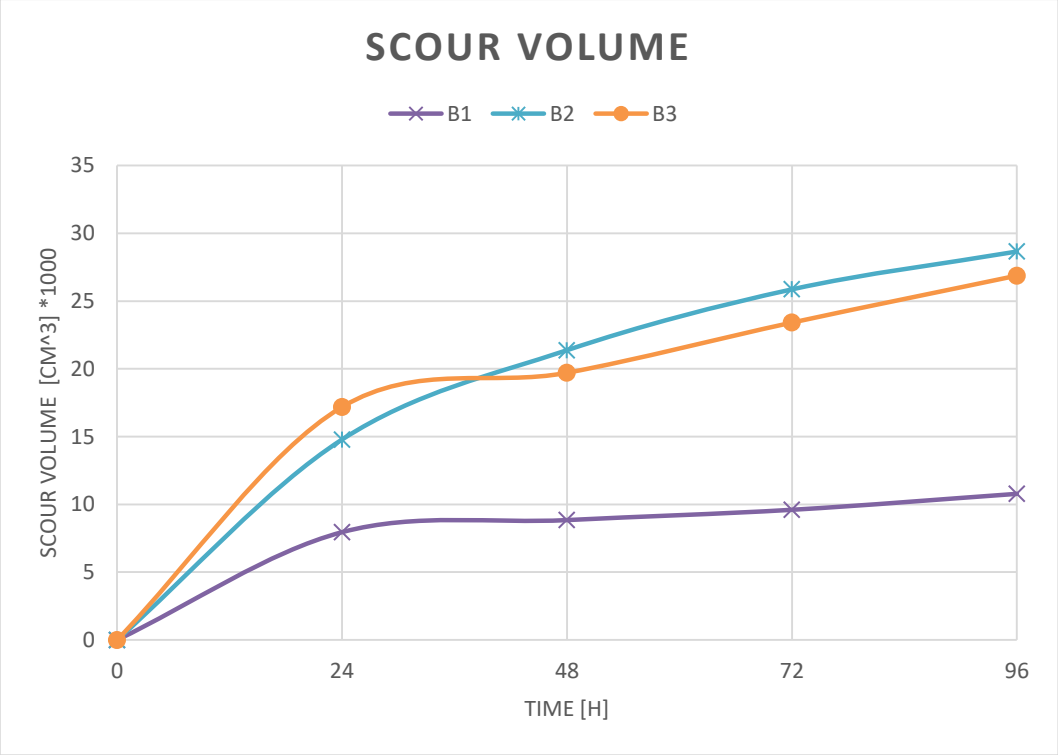

Figure 72; In time scour volume

Table 10; Absolute scoured volume for B-series

Test number	Scour (24h) [cm³]	Scour (48h) [cm³]	Scour (72h) [cm³]	Scour (96h) [cm³]
1	2482	3373	4134	5310
2	6013	12601	17090	19881
3	8997	11515	15218	18682
Average	5831	9163	12147	14624

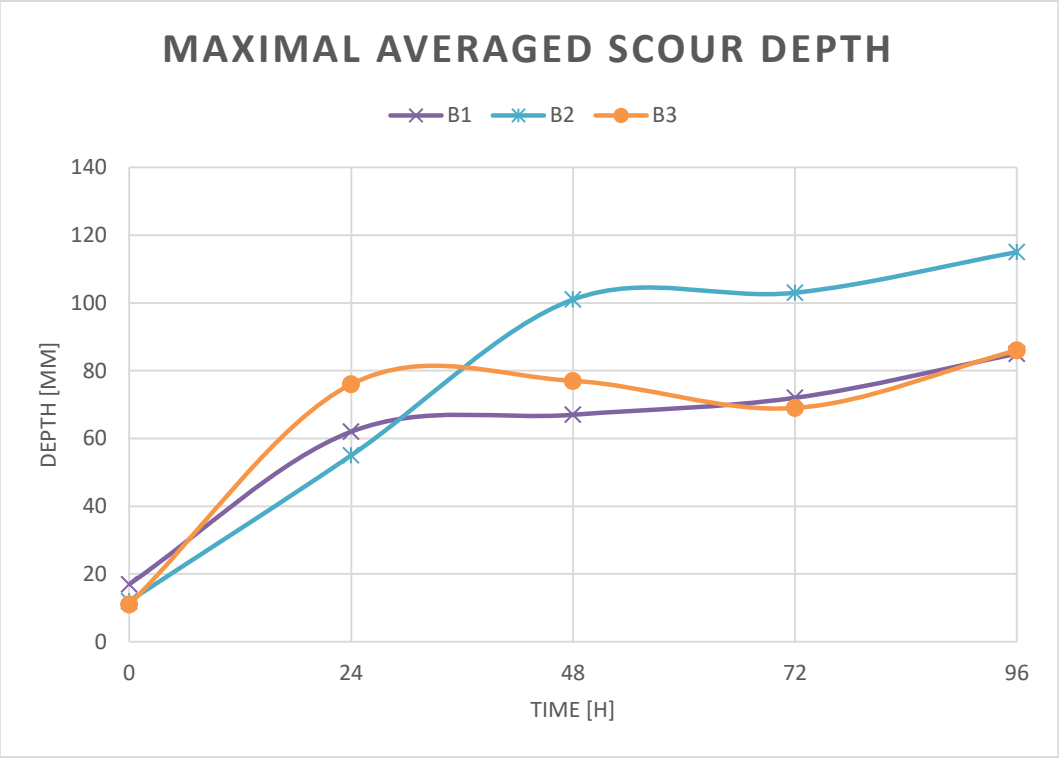

Figure 73; Maximum cross-sectioned average scour depth

For arguments sake, the results of protection scour B1 are henceforth discussed. A complete report for every experiment can be found in Appendix EI, EII & EIII. From the onset of flow, the log layer acts like a vertical step and consequently flow behind the logs is on average upstream directed as can be seen in flow profiles (Figure 74(right) & Figure 75(right)). Additionally, projections of the fluctuation intensity at locations downstream of the log layer (Figure 74(left), Figure 75(left) & Figure 76) show that velocity fluctuations in at these locations are on average as big or bigger than the average velocities that are measured in these areas.

A measurement of the bed shear stresses show that from the start, locations primarily downstream of the logs (6-11) face heavy attack. Values above a magnitude of 0,16 [n/m^2] are associated with scour following the results basic scour experiments, and are thus made red. Locations 4 & 9 are located and measured on top of the log layer, and thus do not represent the actual values near the bed. Scour rates predicted on the basis of these bed shear stresses following the reworked van Rijn formula (equation 8) are depicted in appendices DI, DII & DIII. They predict a mix of transport rates with excessive transport rates often occurring around the logs that greatly exceed visual observations as well as the available supply. Because the sediment transport formula of van Rijn incorporates cross section averaged flow velocities the application of the formula in this situation were the flow profile is severely disturbed is questionable.

Table 11; Bed shear stress at onset of motion [n/m^2] 0 [h] following the Reynolds method specified per location

	1	2	3	4	5	6	7	8	9	10	11
B1	-0,066	-0,071	-0,011	-0,282	-0,022	-0,132	-0,057	-0,059	-0,089	-0,105	-0,219
B2	-0,053	-0,065	-0,077	-0,288	-0,040	-0,203	-0,062	-0,035	-0,121	-0,142	-0,170
B3	-0,046	-0,062	-0,076	-0,619	-0,074	-0,215	-0,062	-0,285	-0,437	-0,217	-0,233

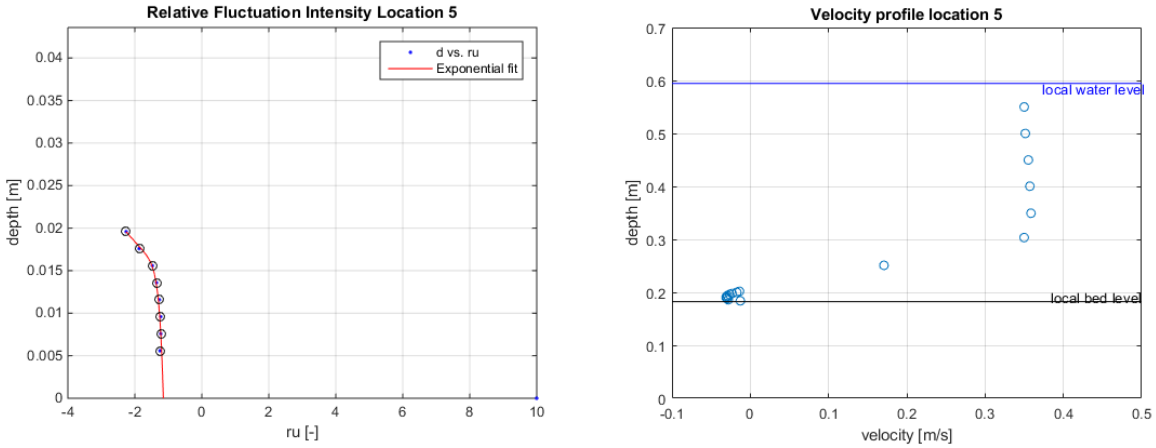

Figure 74; Relative Fluctuation intensity (left) and flow profile (right) for location 5 experiment B-1 at 0 [h]

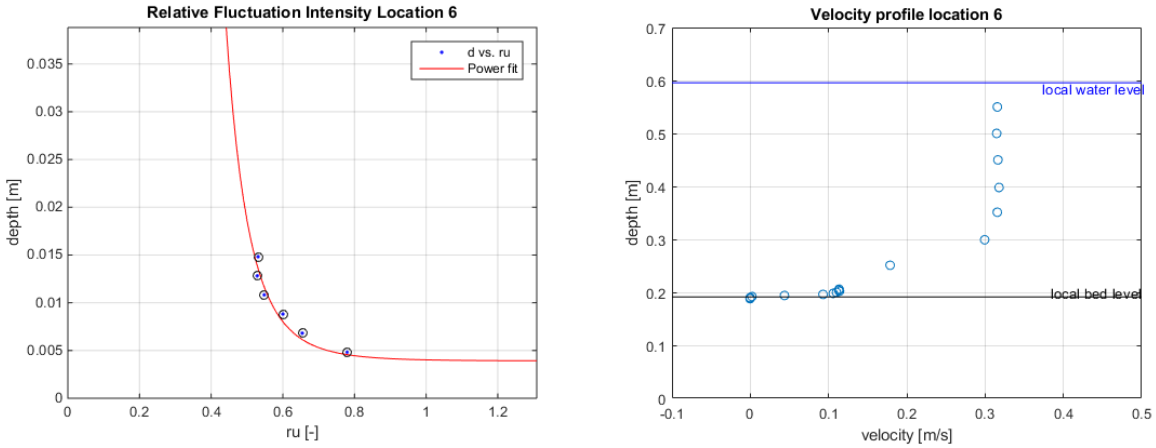

Figure 75; Relative Fluctuation intensity (left) and flow profile (right) for location 6 experiment B-1 at 0 [h]

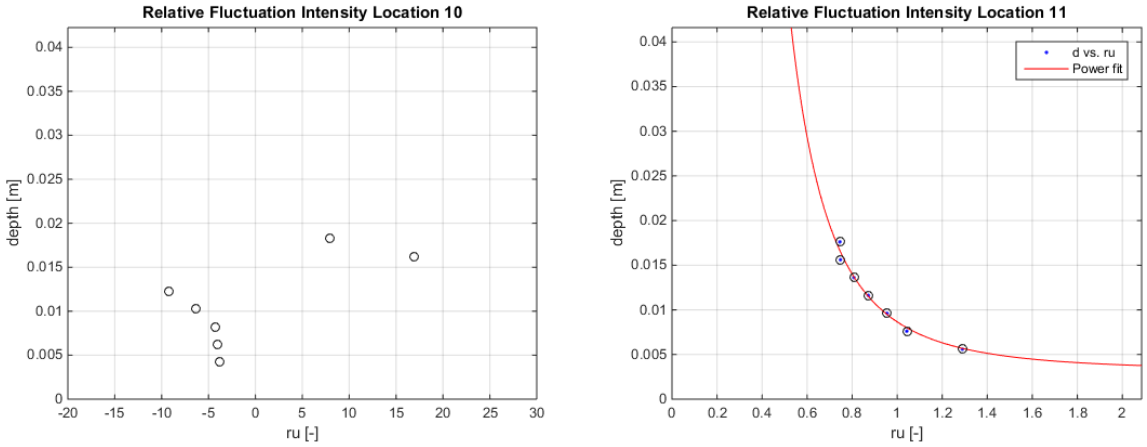

Figure 76; Relative Fluctuation intensity for location 10 (left) and 11 (right) for experiment B-1 at 0 [h]

Figure 77-Figure 81 depict the staircase mechanism that was discussed in section 3.1.2. This mechanism has occurred for all three experiments. Within the first 24 [h] a steep scour hole developing at the upstream face, causes the logs to roll into the scour hole. The bulk of the movement occurs within these first 24 [h], after this time the logs tend to settle a bit more, but movement is limited. Figure 82 shows the in time development of this mechanism in more detail.

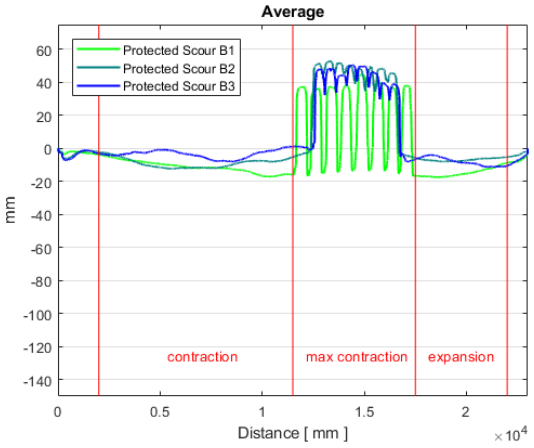

Figure 77; Average transects after 0[h]

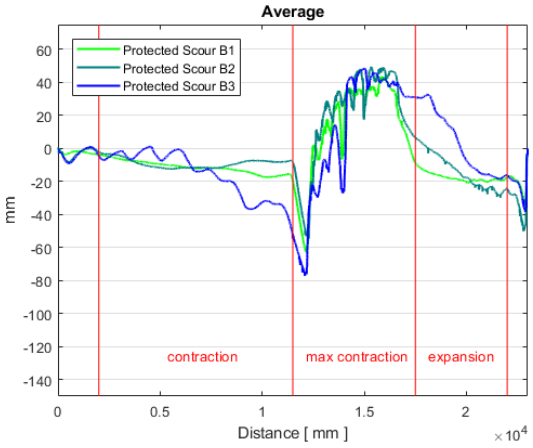

Figure 78; Average transects after 24[h]

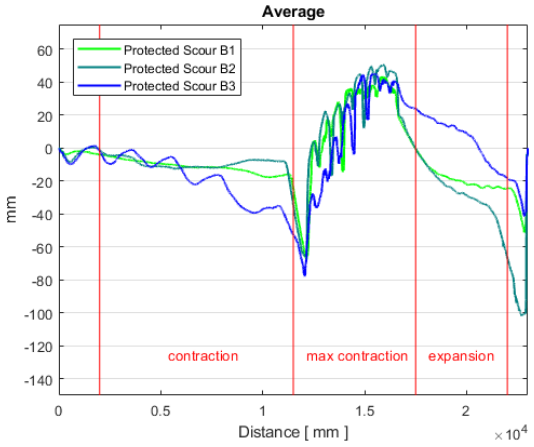

Figure 79; Average transects after 48[h]

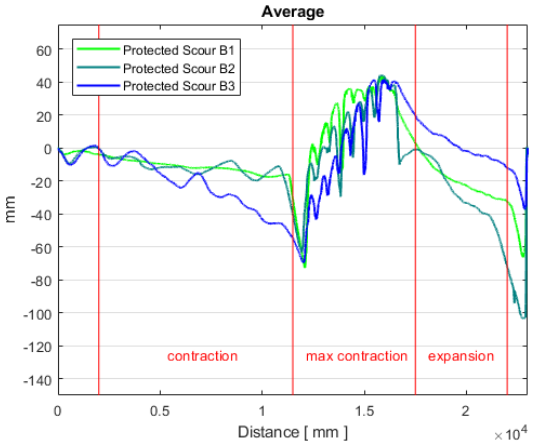

Figure 80; Average transects after 72[h]

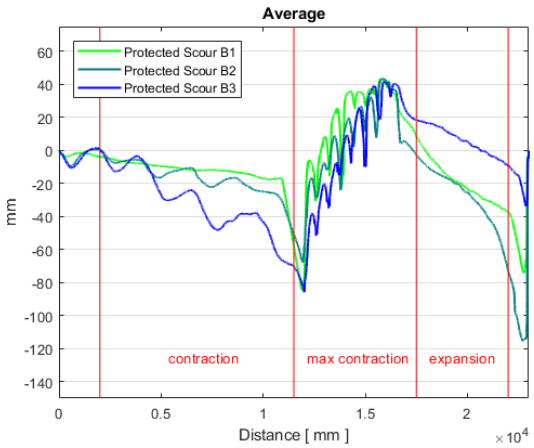

Figure 81; Average transects after 96[h]

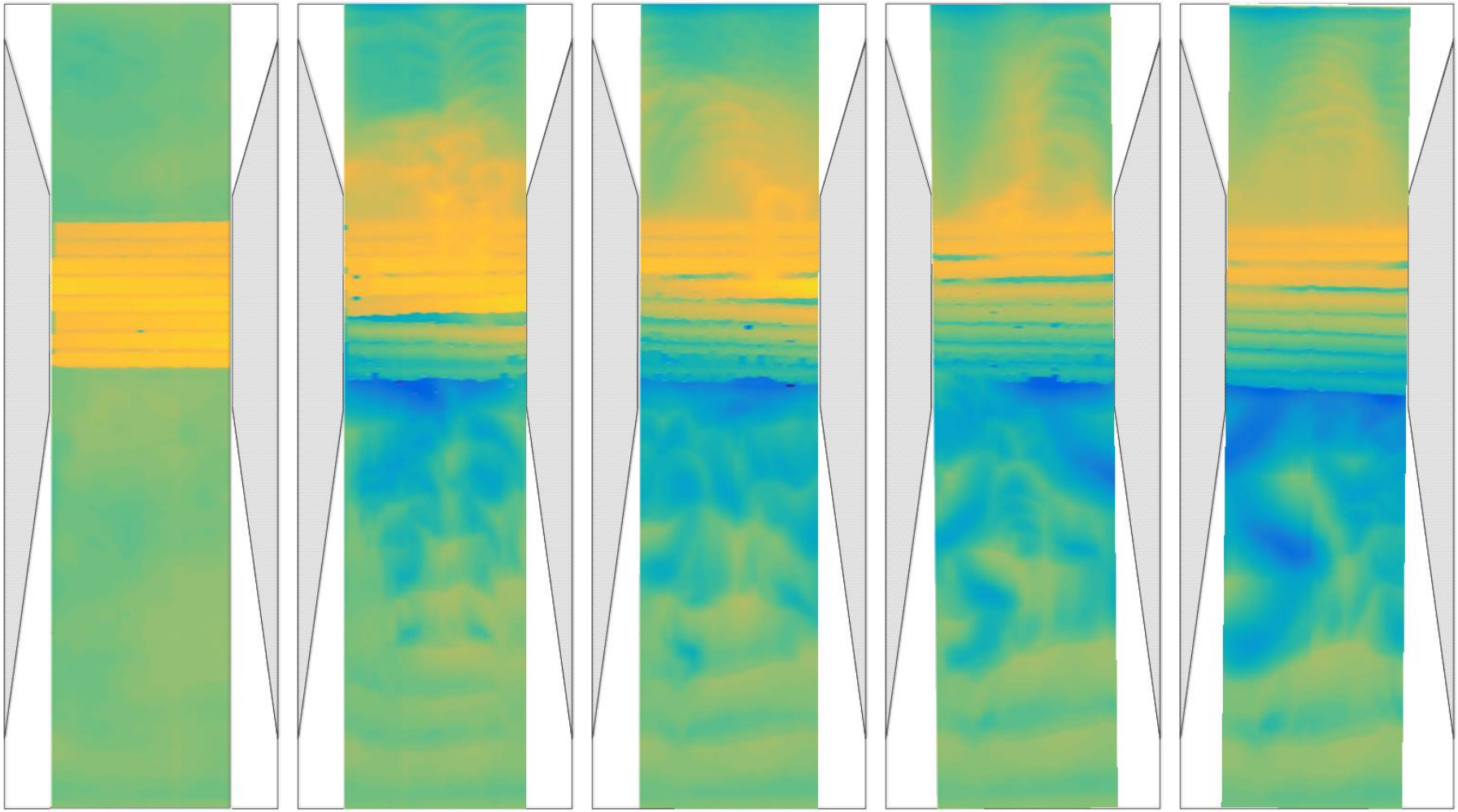

Figure 82; Progression of scour with flow perpendicular placed logs at 24 [h] intervals (Experiment B3)

3.3 Analysis

The cause for scour is distinctly different for both types of experiments, thus they will be discussed separately in this section.

3.3.1 General

Before an in depth analysis can take place, scour quantities require to be corrected similarly to the basic scour experiments. After correcting the experiments to a reference zero elevation bed, and subtracting the volume of the logs (roughly 10,000 [cm^3]) the figures of Table 11 are obtained. This table shows that both series scour roughly the same on average.

Table 12; Relative Scour quantities

Test number	Scour (0h) [cm^3]	Scour (24h) [cm^3]	Scour (48h) [cm^3]	Scour (72h) [cm^3]	Scour (96h) [cm^3]
A1	10063	13350	20820	27737	33174
A2	8146	9871	11779	22419	30819
A3	5467	8701	9885	10227	10108
Average A series	**7892**	**10640**	**14161**	**20128**	**24700**
B1	13117	16393,8	17298	18059	19234
B2	7027	13044	19634,8	24123	26914
B3	5672	14690,8	17209	20912	24375
Average B series	**8606**	**14709**	**18047**	**21031**	**23508**

Comparing the two before mentioned scour experiment series, a few interesting differences are noticeable. Beside the mechanism that is present, it can be observed that experiments that scour relatively small quantities in the contracting or the constriction-sector, tend to develop scouring holes far downstream of the log layer (A3, B1, B2, B3) (Figure 70 & Figure 81). The mechanisms that are causing the observed differences are discussed for each series separately.

3.3.2 Protected Scour Experiments – A series – Flow parallel

The typical development of this type of configuration starts with small circular scour holes underneath the upstream located face of the log layer (Figure 83). These scour holes develop within several minutes. The scouring particles form tiny plumes in between logs and are transported away from the logs as suspended load transport. The mechanism behind this scour phenomenon was also observed in the Burial Scour experiments and is most likely caused by the pier like behavior the log layer assumes. This unfortunately cannot be confirmed with the measurements just upstream of the logs, as the presence of the logs required the measurements to be taken 5-10 [cm] upstream from the logs. In this area bed shear stresses and relative fluctuation intensity do not necessarily exceed values that cause scour Appendix D1, D2 & D3.

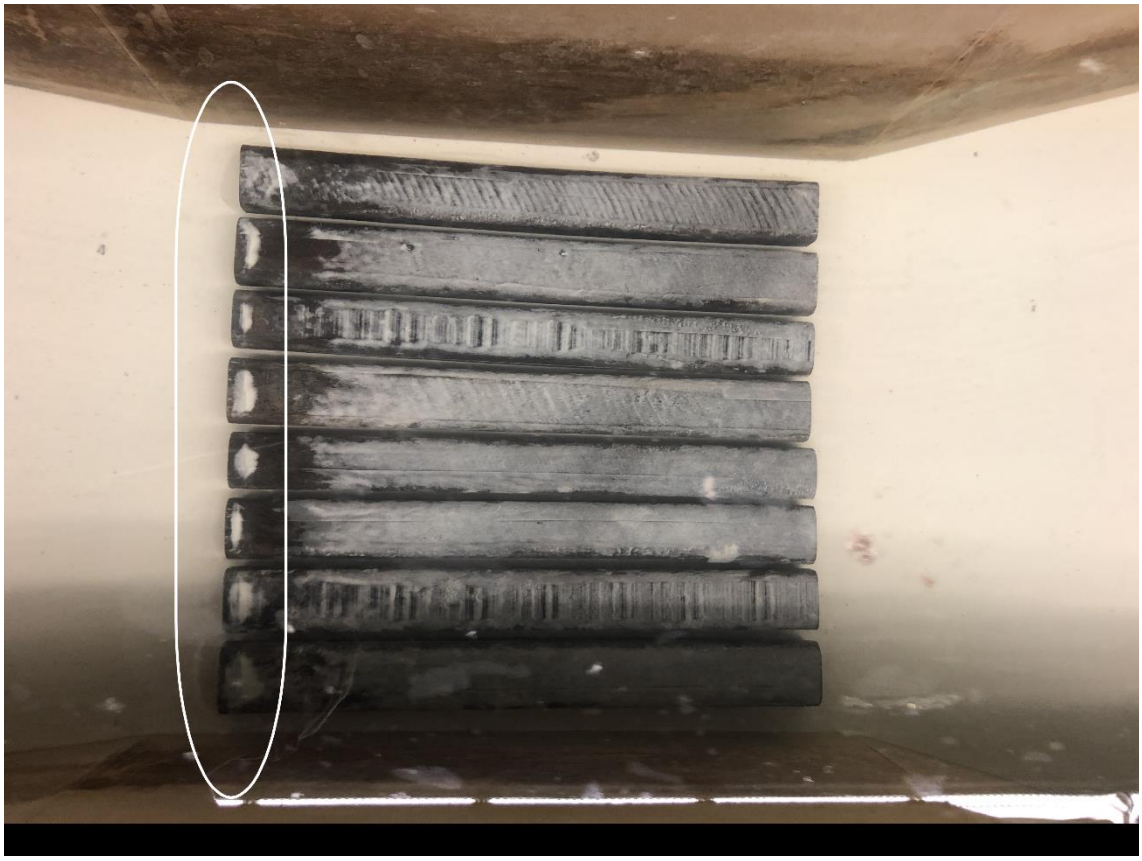

Figure 83; visually observable small indentures under upstream face of log layer

The scour holes underneath the upstream faces of the logs quickly grow to a magnitude that cause the holes to connect and form a uniform trench (Figure 84). Small dunes of sand can be observed to move in between the logs. The cantilever mechanism follows when the scour hole upstream of the logs is large enough to cause them to start to tip over. The presence of the dunes in between the logs has the ability to slow this process down, but the tipping mechanism seems to be inevitable.

Figure 84; Uniform scour hole and migrating dunes

For the experiments that were conducted in this thesis, experiment A3 did not tip sufficiently to activate the final stage of the cantilever scour mechanism. It can be observed that for the first 24 [h] (Figure 85) scour development for experiment A2 almost identical as for A3, with similar maximum scour depth, and position of logs. Tipping however occurred for experiment A2 during the next 24 [h] (Figure 86), from this point scour accelerates. As the A3 experiment log layer does not move much after the first 24 [h] an estimation can be made for what angle of the log layer the third phase of the cantilever mechanism is activated. This is between 8-11 degrees. The exact cause for the third stage not setting is unknown, but it may be expected that given enough time, the mechanism would occur. Observable is that at the measurement taken at 96 [h] (Figure 88), the logs seem to have tipped to almost 9 degrees, dangerously close to the onset of the third phase.

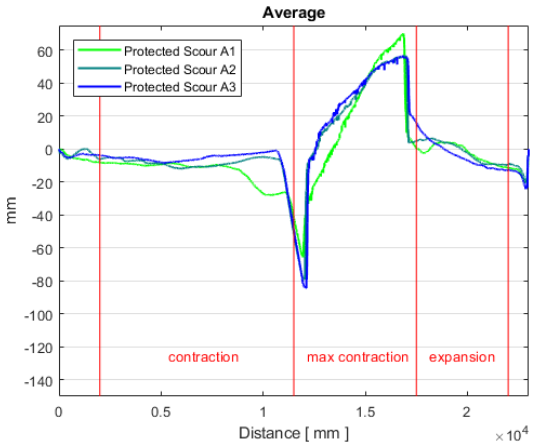

Figure 85; Average transects of A series after 24 [h]

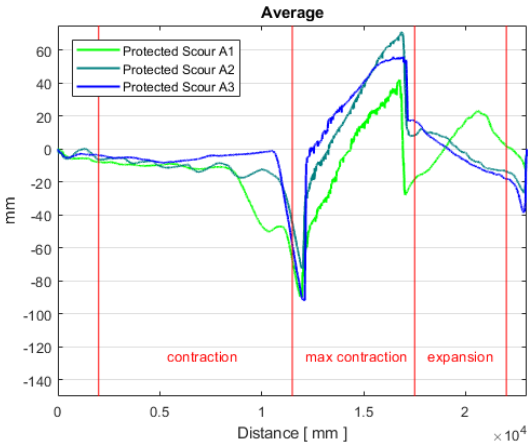

Figure 86; Average transects of A series after 48 [h]

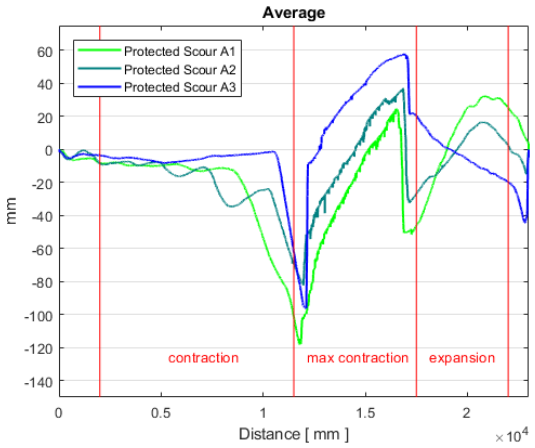

Figure 87; Average transects of A series after 72 [h]

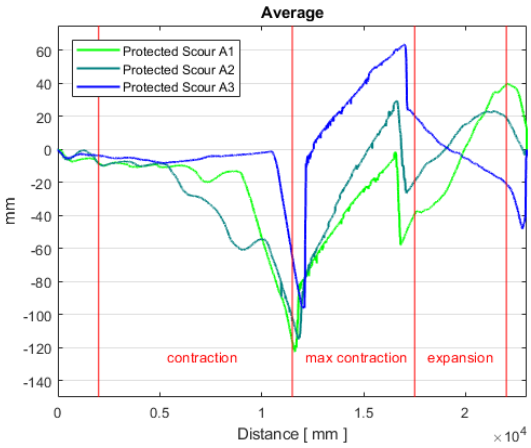

Figure 88; Average transects of A series after 96[h]

The downstream scour hole that was observed for experiment A3 but not for A1 and A2, can be explained through a series of coinciding occurrences. As discussed earlier the logs of scour experiment A3, stopped tipping over (or slowed down significantly), this in combination with dunes of sand stuck in between the logs cause the log layer to behave like a fully formed vertical step. A complex 3-D flow pattern that originally occurred behind the logs has now redeveloped in a 2-D one. Traditionally flow reattachment causes heavy attack 10-20 times the vertical step height downstream of the vertical step (Schiereck and Verhagen 2012). This initially places the flow reattachment point well within the measuring range, but as the logs tip over slightly and the downstream end is raised to 63 [mm]. The flow reattachment point now lies beyond the laboratory model. This is to some respect observable from the bed shear stresses measured at locations downstream of the logs. They initially start to experience high bed shear stresses after approximately 24 [h], but as the logs start tipping and developing a uniform crest, this attack is reduced and consequently sediment transport slows down.

Table 13; Bed shear stress [n/m^2] and sediment transport

Time	0 [h]	24 [h]	48 [h]	72 [h]	96 [h]
Bed shear stress Location 6	-0,124	-0,279	-0,278	-0,110	-
Bed shear stress Location 11	-0,045	-0,129	-0,021	0,030	-
Scour from downstream section [cm^3]	-	573	441	207	143

3.3.3 Protected Scour Experiments – B series – Flow perpendicular

The typical development of this type of configuration starts with small scour holes that originate from the edges of the most upstream located log, the scour holes move towards the center of the most upstream located log. The mechanism at hand resembles pipeline scour mechanisms This would point to strong bed shear stresses at the edges of the logs, this unfortunately cannot be confirmed with the measurements just upstream of the logs because as before, the location of scour was too close to the log.

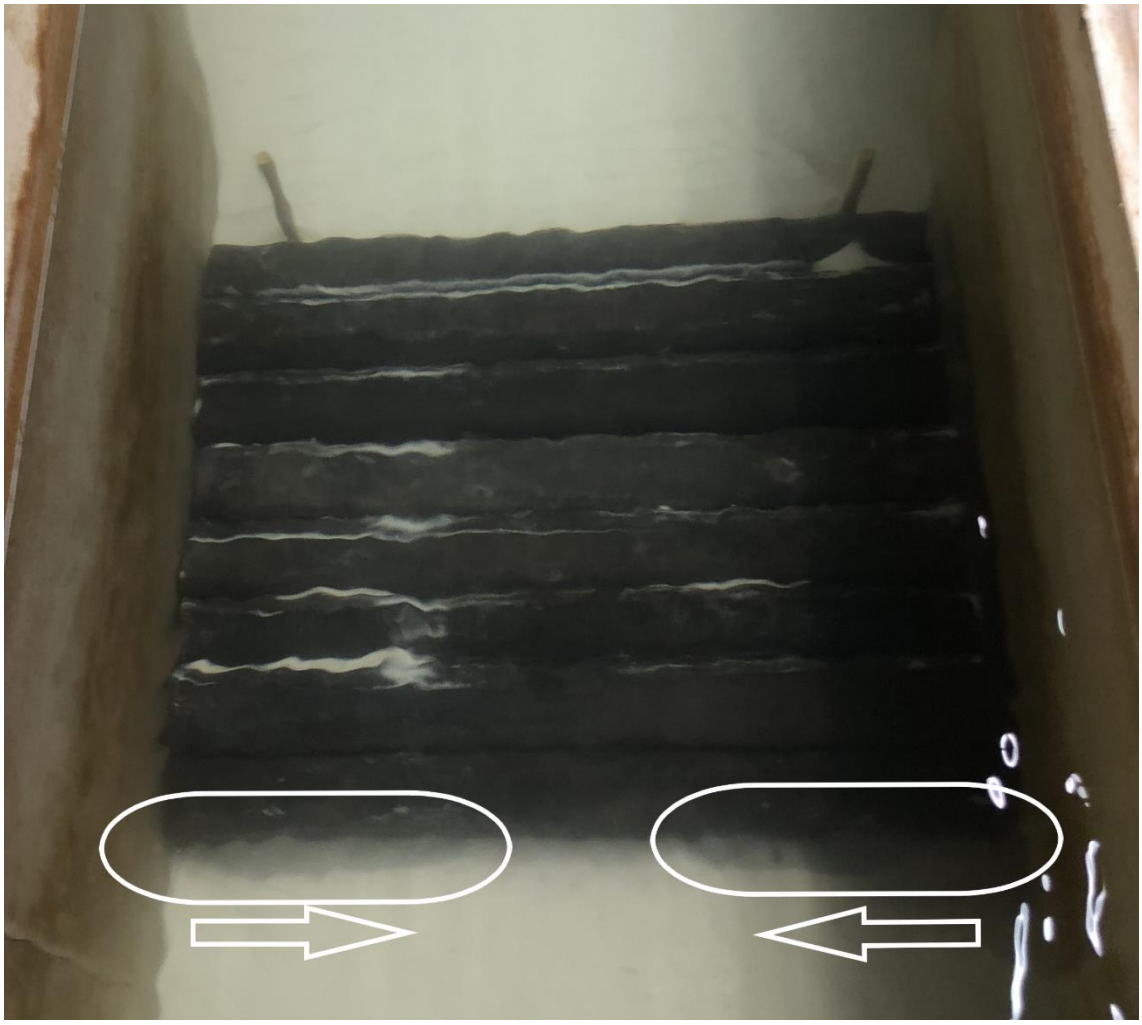

Figure 89; Scour holes migrating towards the center of the most upstream located log

The scour holes slowly expand towards each other to connect and form a uniform trench (Figure 90). Some transport in the form of dunes is observable between the logs and the side walls. The staircase mechanism follows when the scour hole upstream of the logs has expanded enough to cause the first log to roll in. This exposes the slope underneath the first log to flow, and the second and third log quickly follow to connect as a slope of logs.

Figure 90; Uniform scour hole causes logs to roll in

For the experiments that were conducted in this thesis, all experiments reached the final stage of the staircase mechanism, connecting a full slope of logs. Also observable is the fact that for all three experiments, the staircase mechanism is fully activated within the first 24 [h], after which the logs do not seem to show much movement. Figure 91 shows that directly downstream of the logs accretion starts to connect the bed to the logs.

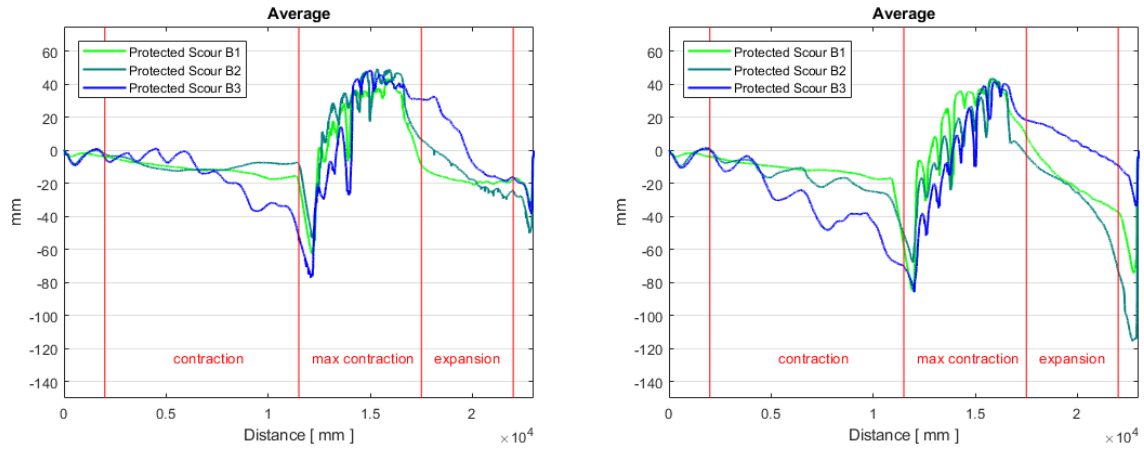

Figure 91; Average transects after 24 [h] {left) and 96 [h] (right)

For all three experiments in the B-series a downstream scour hole was observed. Given differences in magnitude are caused by a combination of geometry of the log layer and upstream sediment import. Observable from figure 86 is that B2 scours relatively little upstream but scour downstream is very large. Experiment B3 on the other hand scours a significant amount of sand upstream and consequently, the downstream scour hole is very small. Experiment B1 does not show much scouring upstream and a relatively deep scour hole downstream of the log layer, although the lack of import would allow one to expect a deeper scour hole. The explanation for this scour hole development is similar to the explanation for experiment A3. Traditionally flow reattachment causes heavy attack 10-20 times the vertical step height downstream of the vertical step (Schiereck and Verhagen 2012). The log layer acts like a fully formed vertical step with near bed negative velocities for all three experiments just downstream of the logs. As the logs are about 45-50 [mm] above the reference bed level, the reattachment point is located near the edge of the measuring range. Figure 92, Figure 93 & Figure 94 show that this can be confirmed, as near bed flow velocities seem to pick up at the locations that are within range of the area that experiences scour. Additionally, Table 14, Table 15 & Table 16 show that for all three experiments these locations continuously experience high bed shear stresses. The transport rates associated with these bed shear stresses are fully discussed in Appendices EI, EII & EII and show that for all three experiments some scour in this section was predicted. Interesting to note is that the values would indicate the downstream sector to be supplied from upstream sectors. This seemingly does not happen and given the import from upstream, the export of sediment from the downstream sector is much larger than bed shear stresses in combination with the van Rijn equation (equation 8) would predict.

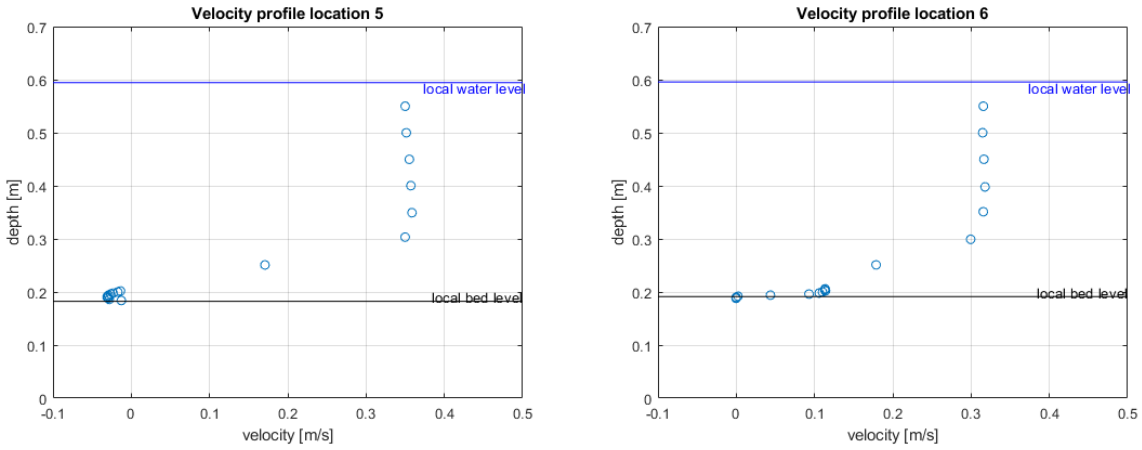

Figure 92; Velocity profiles for location 5 (left) and location 6 (right) for experiment B1

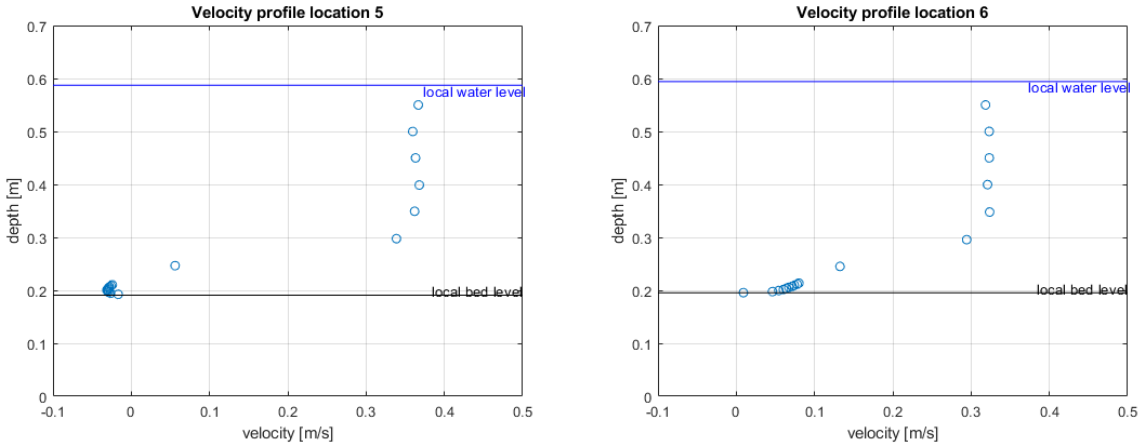

Figure 93; Velocity profiles for location 5 (left) and location 6 (right) for experiment B2

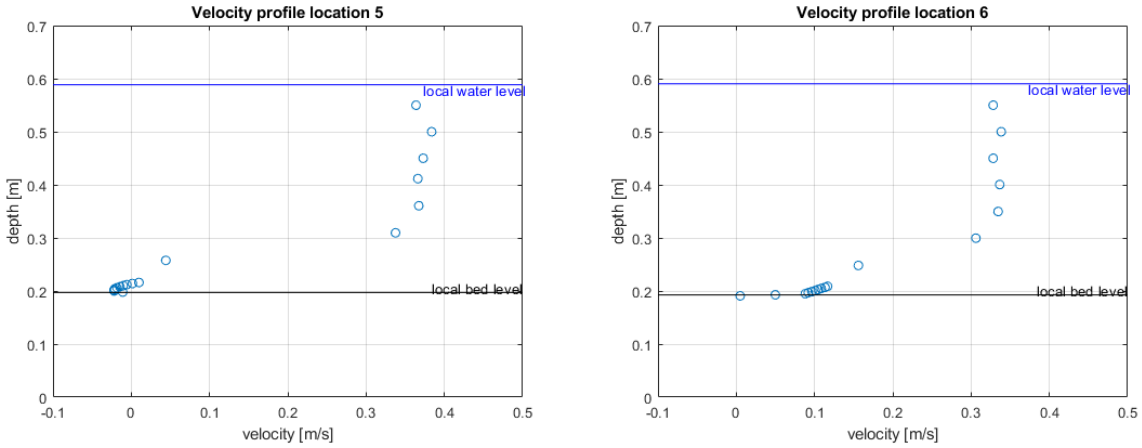

Figure 94 Velocity profiles for location 5 (left) and location 6 (right) for experiment B3

Table 14; Bed shear stress [n/m^2] for experiment B1

Time	0 [h]	24 [h]	48 [h]	72 [h]
Bed shear stress Location 6	-0,132	-0,020	-0,380	-0,086
Bed shear stress Location 11	-0,219	-0,145	-0,140	-0,101

Table 15; Bed shear stress [n/m^2] for experiment B2

Time	0 [h]	24 [h]	48 [h]	72 [h]
Bed shear stress Location 6	-0,203	-0,260	-0,188	-0,321
Bed shear stress Location 11	-0,170	-0,182	-0,235	-0,004

Table 16; Bed shear stress [n/m^2] for experiment B3

Time	0 [h]	24 [h]	48 [h]	72 [h]
Bed shear stress Location 6	-0,215	-0,129	-0,334	-0,418
Bed shear stress Location 11	-0,233	-0,218	-0,010	-0,0123

3.4 Conclusion

From the results of the A & B series of protected scour experiments it can be concluded that the orientation of the log carpet is of significant importance to the scour development. The results show that corrected for initial bed differences both series scour approximately similar amounts of sediment. Maximum scour depths are larger for a log protection with flow parallel logs but the differences are again limited. How these results compare to experiments without logs will be discussed in the next chapter.

4 Comparison of Results

Stated in chapters 1 and 3 are the results from the experiments without a protection of logs and experiments with two different configurations of a log protection. The focus of this chapter will be to compare all series of experiments, and present the reader with conclusions into the application of logs as a scour protection.

4.1 Scour volume

A comparison for the scour volume's corrected to initial bed differences and the presence of logs can be found in Table 17. The table shows that the presence of logs has a significant influence on scour, as scour rates are reduced up to 40%.

Table 17; Scour volume corrected for initial bed differences [cm^3]

	Scour (0h)	Scour (24h)	Scour (48h)	Scour (72h)	Scour (96h)
Average Basic Scour	9607	19566	28336	33199	39506
Average Protected scour A	7892	10640	14161	20128	24700
Average Protected scour B	8606	14709	18047	21031	23508

A side note to be made however, is the fact that for the Protected scour B series this scour for a large part takes place downstream of the logs due to their presence on the bed. The actual application of logs will focus on a placement below existing bed levels, thus the erosion caused by the vertical step will not necessarily take place. Additionally the protected scour A experiments most likely would also cause this scour phenomenon, had the experimental set up have been more elongated. Excluding the downstream-sector from all experiments with logs, results in Figure 95 & Table 18. Note that the logs hanging over a the scour hole for the protected scour A-series, depict a lower scour rate in the first 72 [h] this is most likely not the case or in any case an underestimation of the actual scour quantities. Scour quantities after 96 [h] where determined with a projection of the bed where logs were already removed. With the removal of the scour hole downstream of the logs, it appears that flow perpendicular placed logs provide the best results with a reduction of scour volume of almost 50% followed by the flow parallel logs with a reduction of 40%. If additionally the A-3 experiment is excluded (due to the un developed cantilever mechanism) the scour reduction for flow parallel logs reduces to 18%.

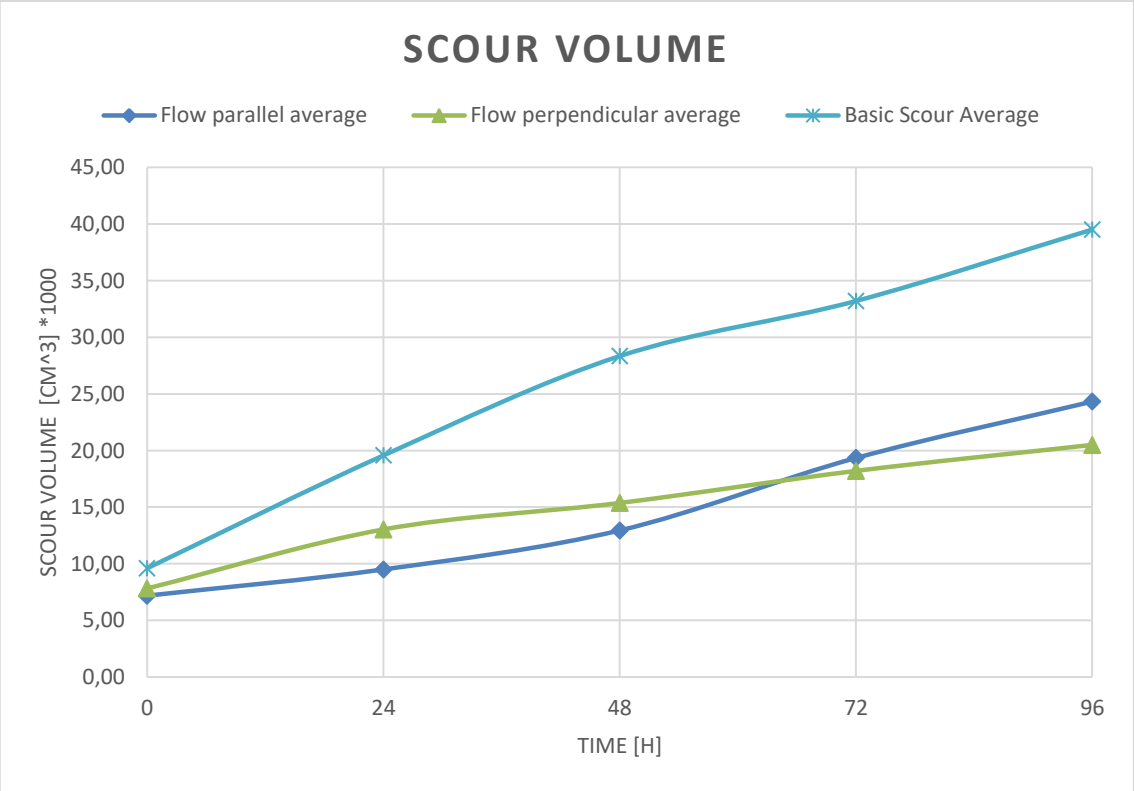

Figure 95; Scour volume graph corrected for initial bed differences and excluding downstream-sector in [cm^3]

Table 18; Scour volume corrected for initial bed differences and excluding downstream-sector in [cm^3]

	Scour (0h)	Scour (24h)	Scour (48h)	Scour (72h)	Scour (96h)
Average Basic Scour	9607	19566	28336	33199	39506
Average Protected scour A	7184	9500	12943	19339	24317
Average Protected scour B	7822	13034	15369	18200	20495

4.2 Maximum scour depth

Another measure of comparing scour is to comparing the maximum cross-section averaged scour depth. The maximal measured cross-section averaged scour depth is visible in Figure 96. It shows that after 96 hours the flow parallel placed logs produce on average the largest scour depths. These are for all A-series experiments located within the constricted-sector, on the upstream face of the log layer. The B-series follows at a distance with an on average scour depth of 95 [mm] after 96 [h]. These scour depths where measured in front of the upstream logs for 2 experiments, and for 1 in the scour hole generated downstream. The basic scour experiments have shown the least maximum scour depth with about 88 [mm] on average.

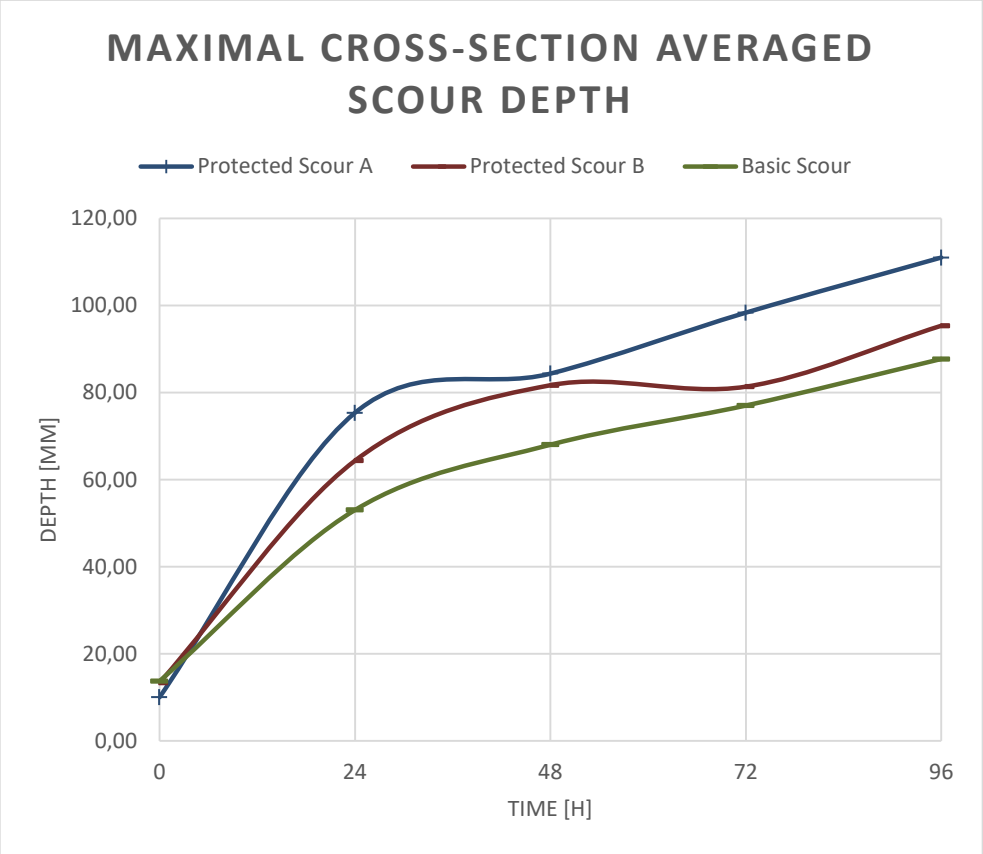

Figure 96; Maximal measures cross-section averaged scour depth

As stated before, the location of maximum cross-section averaged scour hole is not always located near the logs, but also in the scour hole that is generated downstream of the logs. As mentioned earlier, the specific application of logs below bed level, would not cause this scour hole to develop. If only the maximum attained scour depths in the contraction and constriction-sectors is taken into account, Figure 97 is obtained. This figure places the maximum scour depth of the B-series experiments below the Basic scour experiments, with an average scour depth of 80 [mm] after 96 [h].

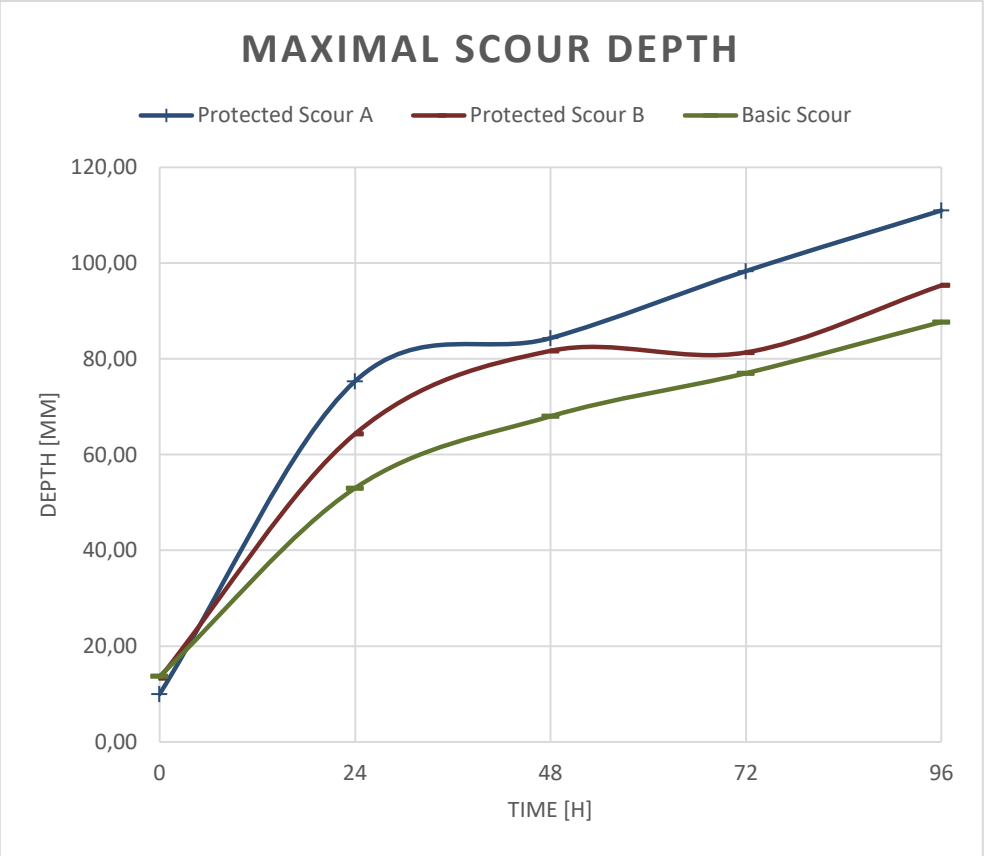

Figure 97; Maximal measures cross-section averaged scour depth excluding downstream sector

Finally comparing the average transects of all experiments combined, Figure 98 can be created. From this figure it is quite easily observable that the logs placed perpendicular have the best effect on the construction sector, reducing scour depths and scour volume. Flow parallel placed logs also have positive effects, but tend to increase the maximum scour depth.

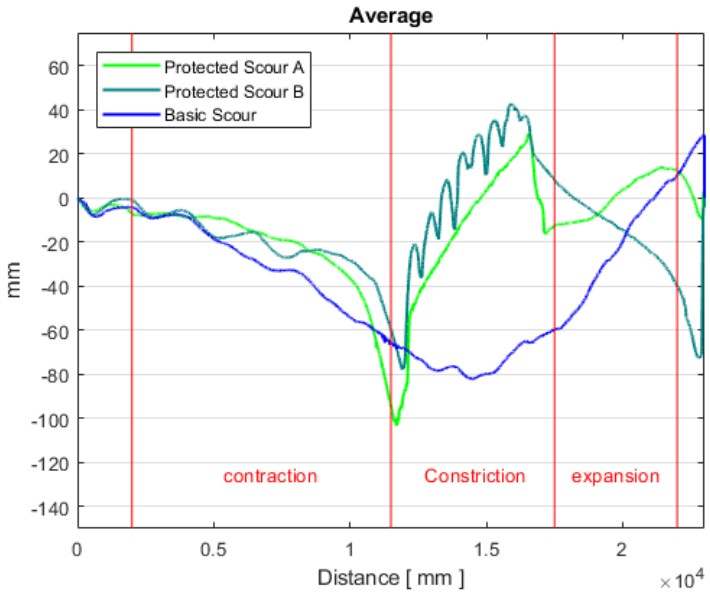

Figure 98; Average transects for all experiments

5. Discussion & recommendation follow up research

This section will include points of discussion for scaling, further experimental inquiries as well as prototype and real world application of a protection with logs. Bullet points will be presented with points of discussion followed by recommendations from the writer.

Experiments

- The first point of discussion with respect to experiments is the manner of application and the amount of layers that were applied. The experiments focused on creating a baseline scenario, only including a single layer placed directly on top of a bed with no bedforms and as smooth as possibly in combination with only applying the layer in the area under the highest loads (situated in the constriction-sector). The first priority for further research would be to diversify these conditions by experimenting with more layers, extended areas of protection and possibly applying the logs on a more natural bed. Also applying the logs in an already partially developed scour hole could be an important step to determining the effect of a protection of logs

- The choice of model scale is a second point of discussion. As was stated earlier, due to a mismatch of scale between the logs and the bed material one might expect a difference is scour depths. Following the theorem from (Lee and Sturm 2009) scour depths are approximately 3% larger than real life would produce. It is however questionable to what extend these bridge pier scour scale relations are applicable to the layer of logs as they have the freedom to move, and are not continuous throughout the water column. The shields scaling principle is in retrospect still considered to be the best way to obtain a gradually forming scour hole. Interesting to note is that the 1:10 scale of the logs and the shields scaling of the flow conditions to the bed material come together rather nicely. The shields scaling resulted in flow conditions that according to the Froude law & the research into the hydraulic resistance (van Olst, van Leeuwen and van der Scheer 2016) did not exceed the critical velocity for the logs to move. Any smaller scale of the logs would have violated this principle while a larger scale wouldn't have allowed for either the logs to be placed perpendicular or the scaling to shields. Furthermore the flow conditions were eventually such that the flow conditions according to Reynolds were still considered to be turbulent. The second priority would therefore be to conduct experiments that utilize a form of shields scaling with logs and a bed material that are more in line with the ratio's in prototype situations.

- A third piece of discussion includes the chosen flow conditions and the resulting clear water scour condition. In reality clear water scour is an ideal scenario, and not necessarily represents all intended locations. Experiments with live-bed scour should be conducted to compliment the knowledge of logs as scour protection. It is however the opinion of the writer of this thesis that of all other points of discussion this has the least priority.

Real world application

- The experiments show that logs cause additional and accelerated scour when positioned on top of a pre-existing bed. This would imply that application of logs below surrounding bed levels would be advisable. As this is also the aim of the existing project it is recommended this line of reasoning is kept if and when application in prototype scenarios becomes viable.

- Comparing the results of the experiments with logs, it is the recommendation of the writer of this thesis that placement of logs perpendicular to the governing flow direction is preferential. Even in situations where the cantilever mechanisms that occurs with flow parallel logs is unlikely to occur. The space between logs will always facilitate transport of sediment between the logs and also canals of potential higher than preferred flow velocities that can cause scour in between the logs to occur.

- When applied perpendicular to the governing flow direction on top of the bed in a clear water scour scenario the Burial scour experiments show that, if possible, the layer should be extended to area's were based on the shields based transport, stage 3-4 is reached. This will cause scour to occur near the logs and activate the mechanism, leaving a large amount of logs to cover the slopes of the developing scouring hole.

- A single layer has already shown to be effective, but a multitude of layers would quite possibly provide a much better protection against scour. With multiple layers it can be reasoned that the staircase mechanisms occurring when logs are placed flow perpendicular would have more logs to fill gaps in between the logs reducing the attack at these locations. With the flow parallel logs the spaces in between the logs will be reduced which might also have a strong positive effect on the development of scour.

- In tidal regions with possible two way flow perpendicular placement is favorable; cantilevering flow parallel logs can cause two way erosion and strong return currents could shift or displace logs. The staircase mechanism occurring when flow perpendicular logs are present is applicable in two directions

- In areas with where logs are exposed to high hydrodynamic loads and bed conditions are relatively smooth flow parallel placed logs have the highest resistance to movement. This was also determined from the experiments conducted by (van Olst, van Leeuwen and van der Scheer 2016)

- In river bends and close to objects the application of logs is prone to extra complications. Complex scour patterns might cause the favorable staircase mechanism not to occur. It is the advice of the writer of this thesis to approach certain locations by only applying the logs beneath the average bed level at such locations.

6. Conclusion

How do scour quantities develop in a chosen laboratory model without the application of logs, and does this concur with the expectations from the hydraulic sciences?

The shields parameter scaling resulted in scour magnitudes that were expected by using the van Rijn method to predict scour rates. Predicted maximum equilibrium scour depths were not reached within the specific chosen frame of time however. But observable is that the maximum scour depths do slowly approach these values.

What is the behavior of a single log on itself and the bed in varying flow conditions?

Given varying flow conditions, logs will have the tendency to firstly behave as a pier like structure, when certain flow conditions are met, logs will turn and start to behave like pipelines.

What matter of log protection application is most appropriate in this model, and how does certain application affect the development of the scour quantities.

A single layer of flow perpendicular placed logs reduce scour quantities for experiments within this particular setting with on average 50%, and reduce scour depths with 8%

Does the scouring process change in such a way that new scouring mechanisms arise and/or start to dominate the scouring process?

A layer of logs, on top of an existing undisturbed bed can cause the formation of a scour hole downstream of the location due to flow reattachment.

What is the effect of the placement of logs as bottom protection, on the in time development of scouring holes?

A layer of logs will cause the scouring process to accelerate in the earliest stages and large scour depths are quickly attained, however, in time scour depths noticeably reduced.

List of Symbols

Symbol	Definition	Unit
$\boldsymbol{B}$	Width	m
$\boldsymbol{B_s}$	Shape correction factor	-
$\boldsymbol{C}$	Chezy coefficient	$m^{0,5}/s$
$\boldsymbol{d_b}$	Soil depth	m
$\boldsymbol{d_s}$	Scour depth	m
$\boldsymbol{D_{15}}$	15% exceedence particle diameter	m
$\boldsymbol{D_{50}}$	50% exceedence particle diameter	m
$\boldsymbol{D_{90}}$	90% exceedence particle diameter	m
$\boldsymbol{D}$	Diameter of logs	m
$\boldsymbol{g}$	Acceleration of gravity	m^2/s
$\boldsymbol{h}$	Water depth	m
$\boldsymbol{k_r}$	(equivalent) roughness of bottom	m
$\boldsymbol{K_\alpha}$	Angle correction factor	-
$\boldsymbol{K_u}$	Velocity correction factor	-
$\boldsymbol{L_l}$	Length of logs	m
$\boldsymbol{n}$	Porosity	-
$\boldsymbol{Q}$	Discharge	m^3/s
$\boldsymbol{r_u}$	Relative fluctuation intensity x-direction	-
$\boldsymbol{r_v}$	Relative fluctuation intensity y-direction	-
$\boldsymbol{r_w}$	Relative fluctuation intensity w-direction	-
$\boldsymbol{s}$	Specific gravity of sand γ_s/γ	-
$\boldsymbol{u}$	Flow velocity in flow direction	m/s
$\boldsymbol{\overline{u}}$	Velocity averaged in time or space in x-direction	m/s
$\boldsymbol{u`}$	Flow velocity fluctuation in x-direction	m/s
$\boldsymbol{u_c}$	Critical velocity	m/s
$\boldsymbol{v}$	Kinematic viscosity	m^2/s
$\boldsymbol{\overline{v}}$	Velocity averaged in time or space in y-direction	m/s
$\boldsymbol{v`}$	Flow velocity fluctuation in y-direction	m/s
$\boldsymbol{\overline{w}}$	Velocity averaged in time or space in z-direction	m/s
$\boldsymbol{w`}$	Flow velocity fluctuation in z-direction	m/s
$\boldsymbol{\rho_h}$	Density wood	kg/m^3
$\boldsymbol{\rho_s}$	Density bed material	kg/m^3
$\boldsymbol{\rho_w}$	Density water	kg/m^3
$\boldsymbol{\sigma}$	Surface tension	$n/\ m$
Δ	Relative density (=$(\rho_s - \rho_w)/\rho_w$)	-
Ψ_c	Shields stability parameter	-

Bibliography

Breusers, H. N.C., and W. H.P. Schukking. *Begin van beweging van bodemmateriaal.* Delft: Hydraulic Laboratory, 1971.

Ettema, Robert, Bruce W. Melville, and Brian Barkdoll. "Scale Effect in Pier-Scour Experiments." *Journal of hydraulic engineering*, 1998: 4.

Ettema, Robert, Bruce W. Melville, and Brian Barkdoll. "Scale Effect in Pier-Scour Experiments." *Journal of Hydraulic Engineering*, 1998: 639-642.

Haage, S., and C. Çete . *Bodembescherming met behulp van boomstammen.* Delft: TUDelft, 2016.

Hoffmans, G.J.C.M., and H.J. Verheij. *Scour Manual.* Rotterdam: A.A. Balkema, 1997.

Lee, Seung Oh, and Terry W. Sturm. "Effect of Sediment Size Scaling on Physical Modeling of Bridge Pier Scour." (ASCE) 135, no. 10 (2009).

Melville, Bruce W., and Stephen E. Coleman. *Bridge Scour.* HIghlands Ranch: Water Resources Publications, LCC, 2000.

Micro-Epsilon Messtechnik. "Assembly Instructions optoNCDT 1302." Ortenburg, 1 2 2018.

Mutlu Sumer, B, and Jørgen Fredsøe. *The mechanics of scour in the marine environment.* Singapore: World Scientific Publishing, 2005.

NortekUSA. *Vectrino II 3D profiling Velocimeter.* NortekUSA.

Rijkswaterstaat. *Korte verkenning plaatsing hout Haringvliet/Hollands Diep tbv inventarisatie KRW maatregelen 2de tranche.* Utrecht: Rijkwaterstaat, 2016.

Schiereck, Gerrit J., and Henk Jan Verhagen. *Introduction to Bed, bank and shore protection.* Delft: VSSD, 2012.

Sibelco. *Sibelco/Producten/Kwartszand.* 1 5 2017. www.sibelco.be (accessed 5 1, 2017).

Soulsby, R. *SDynamics of marine sands.* UK: Thomas Telford, 1997.

Stenfert, Joost. *Scour holes in heterogeneous subsoil.* Delft: Delft University of Technology, 2017.

Sterling Jones, J. "Comparison of Prediction Equations for Bridge Pier and Abutment Scour." *Transport Research Record*, n.d.: 202-209.

Sutherland, James, and Richard Soulsby. *Guidelines for physical modelling of mobile sediments.* Barcelona: HR Wallingford, 2010.

van Olst, L., P. van Leeuwen, and B.H. van der Scheer. *Bodembescherming met behulp van boomstammen.* Delft: TUDelft, 2016.

van Rijn, L.C. "simple general formulae for sand transport in rivers, estuaries and coastal waters." *Leo van Rijn.* 20 Febuary 2018. www.leovanrijn-sedimetn.com.